STUDY OF HIGH HARMONIC GENERATION BEYOND DIPOLE APPROXIMATION

Submitted by

Rajeev Mishra

Adviser: Dr. Ashish K. Gupta

DEPARTMENT OF CHEMISTRY

INDIAN INSTITUTE OF TECHNOLOGY

GUWAHATI-781039, INDIA

May 2010

STUDY OF HIGH HARMONIC GENERATION BEYOND DIPOLE APPROXIMATION

A research thesis submitted to the Senate of I. I. T. Guwahati

In partial fulfillment of the requirements for the degree of

DOCTOR OF PHILOSOPHY (Ph. D.)

by

Rajeev Mishra

DEPARTMENT OF CHEMISTRY

INDIAN INSTITUTE OF TECHNOLOGY, GUWAHATI

ASSAM, INDIA

2009

Dedicated to my Parents

Indian Institute of Technology, Guwahati

Guwahati 781039.

Department of Chemistry

STATEMENT

I do hereby declare that the matter embodied in this thesis is the result of investigation carried out by me in the Department of Chemistry, Indian Institute of Technology Guwahati, India under the supervision of Dr. Ashish K. Gupta.

In keeping with the general practice of reporting scientific observation, due acknowledgements have been made wherever the work described is based on the findings of other investigators.

Rajeev Mishra, May 17, 2010

IIT Guwahati

Indian Institute of Technology, Guwahati

Guwahati 781039.

Tel: 0361 258 2312

Fax: 0361 258 2349

E-mail: gupta@iitg.ernet.in

Dr. Ashish K. Gupta

Assistant Professor, Department of Chemistry

CERTIFICATE

It is certified that the work contained in the thesis entitled **Study of High Harmonic Generation Beyond Dipole Approximation** by Rajeev Mishra, a student in the Department of Chemistry, Indian Institute of Technology, Guwahati for the award of degree of Doctor of Philosophy has been carried out under my supervision and that this work has not been submitted elsewhere for a degree.

Dr. Ashish K. Gupta, May 17, 2010

Supervisor IIT Guwahati

Indian Institute of Technology, Guwahati

Guwahati 781039.

Department of Chemistry

CERTIFICATE OF COURSE WORK

This is to certify that Rajeev Mishra has satisfactorily completed all the courses required for the Ph.D. degree program, These courses include

CH 621: New Reagents for Organic Synthesis

CH 605: Applied Crystallography

CH 638: Time Dependant Quantum Mechanics

CH 630: A fundamental approach to Physical Chemistry

Rajeev Mishra has successfully completed his Ph.D. qualifying examination in April 2006.

Professor Arun Chattopadhyay
Head
Department of Chemistry
IIT Guwahati,

Professor T. Punniyamurthy
Secretary
Departmental Post Graduate Committee
IIT Guwahati

Abstract

The thesis entitled, "Study of high harmonic generation beyond dipole approximation" is divided into six chapters. The details of different chapters are as follows,

Chapter 1, gives a brief introduction regarding the pedagogical background as well as literature survey of High Harmonic Generation (HHG) and in addition a general state-of-art of the existing literature on various aspects related to the above mentioned topic is covered. HHG is a process in which usually noble gas atoms when excited by an intense laser field at frequency ω emit radiation of higher frequencies that are usually odd integer multiples of ω. Driven by an infrared laser, high harmonic radiation can span from optical frequency upto extreme ultraviolet (XUV) frequency range. HHG is a coherent, directional, and short-pulsed source of XUV radiation, whose applications include the time-dependent XUV spectroscopy and XUV interferometry. In recent years it also has been exploited to study the orbital shape and molecular properties. HHG gives a deep insight about molecular structure since the recombination step produces coherent emission, and recombination probability depends strongly on initial state electronic wave function. In addition, the harmonic radiation is an excellent seed for a soft X-ray laser. The generated beam being coherent, follow the similar properties of laser light. This chapter also describes the widely used three step process (Ionization, Propagation and Recombination) during HHG mechanism.

In chapter 2 and 3, We have presented formulation and methology used in this thesis and a study of high harmonic generation with model system of the polyacetylene irradiated with intense, linearly polarised (perpendicular to the system axis) laser field propagating along the system axis. Only odd order harmonics will be produced within dipole approximation due to dynamical symmetry of the system but all harmonics (odd as well as even order) are expected in the case of beyond dipole approximation. The validity of dipole approximation is studied as a function of number

of monomer units in the system which can be quantified by comparing intensity, of even harmonics to odd harmonics. The intensity difference between odd harmonics and even harmonics is strongly dependent on number of monomer unit of ethylene taken and the intensity of applied laser field e.g. in case of high intensity of laser field and higher number of monomer units of ethylene, even harmonics become more intense than odd harmonics. It is observed that even if electron oscillation is confined to a small region, non dipole term can not be ignored.

Within DA, due to dynamical symmetry we must get only odd order harmonics. But we expect to get the both (even as well as odd order) kind of harmonics in the case of beyond dipole approximation depending upon the extent of breakdown of DA. The validity of the DA can be checked by observing the intensity of dipole forbidden even harmonics.

In chapter 4, We have studied spectral entropy during the process of HHG. Entropy relates to the fluctuation of population in different states. The entropy (S) of the system is defined as,

$$S = \sum |p_i| log(|p_i|). \tag{1}$$

where $p_i's$ are the population of the electron in i^{th} molecular orbitals. As in previous chapter we have considered the same model system of polyethylene irradiated with intense, linearly polarised laser field propagating along the system axis.

There is no change in maximum spectral entropy in the case of within DA. But it is observed that maximum entropy of the system increases continuously when calculated in the case of beyond DA regime. With this study we have attempted to understand the mechanism of HHG from model system of polyethylene discussed in the previous chapter. In the case of within DA the ground state couples only with single excited state. Hence p_i remain non zero for these two states . But strictly remain zero for other states. But in the case of beyond DA, multipoles will couple all the states, and gives a separate mechanism for population fluctuation among the molecular orbitals p_i even

though small, become significant for the dipole forbidden states which contributes to increase in entropy in the case of beyond DA. This increase in entropy is responsible for producing even harmonics. As the entropy increases, the even order intensity increases without affecting the odd harmonic intensity.

In chapter 5, We present here an investigation of High Harmonics Generation (HHG) from Carbon Nanotube (CNT) using a high intensity CW laser. Here for Linearly polarised (LP) light, due to dynamical symmetry (DS) we should get only allowed harmonics (odd order, when emitted light is polarized in Y direction, and even order, when emitted light is polarized in X direction). And in the case of beyond dipole approximation, one should get all the harmonics irrespective of polarization direction of emitted light. Whereas, if a circularly Polarised (CP) laser light is used, again due to dynamical symmetry we should get only allowed harmonics [$\Omega = (5n \pm 1)\omega : n = 1, 2, 3.....$, where ω and Ω are the fundamental and harmonic frequencies] in both the cases. We have derived the selection rule for generated light polarized perpendicular to the incident laser light.

In chapter 6, We have presented here a study of optimization of high order harmonic generated in two different case of (a) within dipole approximation and (b) beyond dipole approximation. We have considered model system of the ethylene irradiated with intense, linearly polarised (perpendicular to the system axis) laser field propagating along the system axis. It is found that although harmonic intensity increases in both the cases but optimization is always higher in the case of beyond dipole approximation. Study of optimization of even order harmonics as well as odd order harmonics have been done.

Seventh and the last chapter will comprise the summary of the thesis by combining all of the above chapters succinctly and coherently.

Preface

In this thesis, High Harmonic Generation (HHG) Beyond Dipole Approximation (DA) as well as HHG within DA have been investigated. We have studied the the process with polyethylene and carbon nanotue (CNT) system. Along with the HHG study, Entropy during HHG have also been studied. Finally we have optimized the selected harmonic with adaptive control using an evolutionary search process.

Acknowledgments

I would like to thanks to all those people who have contributed to this work directly or indirectly. I learned the theories and concepts involved in high harmonic generation from my guide Dr. A. K. Gupta and he motivated me to extend these HHG studies in beyond dipole approximation regime, for which we found a model system of polyethylene suitable in first sight because of symmetry property. It took four year to find the problem and complete the study of high harmonic generation. In addition to my guide I would like to thanks my doctoral committee members Prof. Arun chattopadhayay, Prof. Alika khare, Dr. P. K. Iyer for their valuable guidance and moral support. The supporting staff of I. I. T. Guwahati have made sure I have gotten paid. Finally, my adviser Dr. A. K. Gupta have spend untold hours advising me and committed undue resources to allowing me to complete my studies.

Contents

Chapter 1

Introduction

1.1 High Harmonic Generation (HHG)

If a very intense laser light of frequency ω strikes atom (with energy $\hbar\omega$) and emits photons with energy $n \times \hbar\omega$ the process is known as harmonic generation and the emitted frequency as the n^{th} harmonics.In 1993 Kulander and Corkum provided a theoretical explanation of high harmonic generation and the similar phenomena of above threshold ionization and non sequential ionization. They explained high harmonic generation in terms of a three step model (discussed later). First, the atom the atom of atomic gas are ionized at roughly the peak of optical cycle. Second, the ionized electron, now in continuum with no kinetic energy, is accelerated by the optical field. When the optical field changes direction, the free electron is accelerated back toward the parent ion. Third, when the electron returns to the parent ion it can do three things: a radiative transition to the ground state, inelastic scattering or elastic scattering. The radiative transition results in High Harmonic Generation (HHG). The inelastic scattering is called non sequential ionization, where the returning electron knocks an additional electron from the atom. Finally, elastic scattering results in very high energy electron in the above threshold ionization spectrum. Based on

simple classical electron trajectories in the optical fields, the returning electron has a plateau of kinetic energies which is then manifest in the high harmonic spectrum. In other words high harmonic generation (HHG) is a process in which usually noble gas atoms excited by an intense laser field at frequency ω emit radiation of higher frequencies that are usually odd integer multiples of ω. Driven by an infrared laser, high harmonic radiation can span from optical frequency into extreme ultraviolet (XUV) [1, 2] frequency range.Harmonics, in the strict sense are generated when the ionization and re-collision are repeated at each laser pulse. Beyond the understanding of the fundamental principles which are at the origin of the harmonic generation process, a strong effort is devoted to its optimization, that is having the strongest conversion efficiency from the laser energy to the harmonics and having the most energetic photons in order to achieve the extreme ultraviolet (XUV) spectral region. HHG is a coherent, directional, and short-pulsed [3] source of XUV radiation, whose applications include the time-dependent XUV spectroscopy and XUV interferometry. In addition, the harmonic radiation is an excellent seed for a soft X-ray laser.

1.2 Literature survey

In a relatively weak laser field the harmonic yield decreases as harmonic order increases. In a higher laser intensity region the harmonic intensity first decreases then reaches a plateau, followed by a sharp cutoff. The plateau has been extended up to 300^{th} harmonics with emitted photon energy more than 500 eV. Thus coherent, ultra-fast pulse, low divergence X-ray beam is generated. Generally in gas media only odd harmonics are generated, but with solid surfaces both even as well as odd harmonics are generated because the surface have no inversion symmetry. Due to symmetry reason high harmonics can be generated using noble gases with elliptically polarized light, but not with circularly polarized light.

Harmonic generation is a highly non-linear [4–6] process in which electric field generated by individual atoms are added coherently, this is known as phase matching [7, 8]. The major limitation of HHG as a coherent light source has been its low conversion efficiency. In particular, ionized electrons in HHG make the media absorbent and dispersive, which leads to the reduction of coherent length over which harmonic radiation can grow because of ionization of gas don't allow the laser and EUV [9], light from propagating with same speed. This problem is overcome by using quasi-phase matching [2, 10–13]. Kapteyn and coworkers showed enhanced generation of coherent light in the "water window" region of soft x-ray spectrum at 4.4 nm, using quasi phase matched frequency conversion of ultra-fast laser. Quasi-phase matching (QPM) is a widely used technique in visible nonlinear optics. In materials where perfect phase matching is not possible, QPM makes it possible to obtain significant conversion efficiency in a nonlinear process by periodically varying the non-linear susceptibility of a material. Therefore developing schemes for QPM is critical in extending efficient HHG conversion to soft-X-ray and shorter wavelengths. Further enhancements are possible using a longer train of counter propagating pulses, allowing the coherent addition of HHG over a longer distance.

The harmonic intensity depends on various parameters, such as; Driving laser field, Focusing, Ionization, Intensity, Phase variations of the atomic dipoles. It was found that the spatial and spectral coherence of HHG depend strongly on the focusing geometry. These properties can be controlled and optimized by moving the laser focus position relative to the nonlinear medium. There are many ways to enhance the HHG, such as pressure, strong static magnetic field, strong static electric field increasing non linearity [4, 5] , multicolor laser, phase matching [2, 10–13], polarization, proper orientation [14], using mixture of gases (Xe + He) [4, 5] and shorter pulses [3]. Using genetic algorithm [15, 16], HHG can be optimized with respect to the different variables.

The highest photon energies obtained from high harmonic generation (HHG) have generally been limited not by the cutoff rule, but by detrimental effects of ionization when using high laser intensities. The resulting plasma can defocus the laser beam, limiting the peak intensities and therefore pondermotive energy (U_P time averaged kinetic energy of electron). It also causes a significant phase velocity mismatch between the driving laser and the harmonic light, greatly reducing the harmonic signal. Ionization can be kept to a minimum by using shorter-duration laser pulses or atoms with a large ionization potential, thus allowing the atoms survive to high laser intensities before ionizing. The highest harmonics observed to date, at around 950 eV, have been generated using helium, which has the largest ionization potential of the noble gases. However, helium also has an exceptionally small effective non linearity [4, 5], which limits the harmonic flux. Larger, multi-electron atoms such as argon typically generate greater signals, but the highest observable harmonic orders have been comparatively lower. For example in Ar, photons of greater than 100 eV energy have never been observed using an 800 nm driving laser even using very short 7 fs duration pulses or large pulse energies. Also, a longer-wavelength driving laser was used to increase the harmonic emission in Ar to around 150 eV. Using longer wavelengths increases the value of U_P for the same laser intensity. However, this approach also reduces the efficiency of the process since the electron wave function is more delocalized, lowering the probability of recombination. Harmonic emission from neutral atoms is limited by the saturation intensity, or the intensity at which about 98 percent of the atoms are ionized. However, emission from ions can in theory extend to very high energies, since the saturation intensity for each successive stage of ionization is progressively higher.

High harmonics are generated by focusing intense laser light into a hollow-core waveguide filled with low pressure gas. The waveguide has several advantages over a gas jet. It counteracts the effect of plasma-induced defocusing, allowing high laser

intensities to be achieved in a fully ionized gas medium. Also, using a modulated-diameter waveguide, the large phase mismatch associated with ionization can be partially compensated by quasi-phase matching. As a result, they observed harmonic generation from argon up to 250 eV, an extension of 100 eV over previous results using a gas jet setup for HHG. These results demonstrate that emission from ions can greatly increase the photon energies obtainable from HHG and that large ions such as Ar, with high nonlinear [4, 5] susceptibilities compared to He, can be used to generate harmonic emission at energies above 200 eV, in the soft x-ray region of the spectrum.

It has been observed that reducing the gas pressure in the waveguide will lead to an increase in the highest observed photon energy. When the argon pressure is increased above 9 Torr, the output mode breaks up and harmonics are no longer observed. Therefore, there exists a limit to the amount of ionization induced defocusing for which the waveguide can compensate. At lower pressure, the flux at lower photon energies is reduced, but at higher photon energies are enhanced. It is possible that there is still some defocusing effect which increases with higher pressures, reducing the intensity. Also, at higher gas pressures, the laser energy at the output of the fiber is reduced, either from ionization or from other loss mechanisms in the waveguide. The reduction in laser energy and therefore intensity could also explain the decrease in harmonic energy.

The laser intensities required to generate the highest harmonics are above the saturation intensity for neutral Ar atoms of $7.5 \times 10^{14} W cm^{-2}$, for an 18 fs laser pulse. Thus highest harmonics are attributed to emission from Ar ions, in the energy range from 160 eV to 250 eV. As we know for the highest energy that can be emitted is given by $E_{max} = h\nu_{max} = Ip + 3.17Up$, where Ip is the ionization potential and Up is podermotive energy of the free electron. Ip of Ar is 15.8 eV. but Ip for Ar^+ is 27.6 eV, which would shift the harmonic energies higher for the emission from

ions with respect to emission from neutral atom. At a laser intensity of around $7.7 \times 10^{14} W cm^{-2}$, Ar is fully ionized, and the highest observable harmonics should therefore be approximately 160 eV. Near the peak of the pulse, the rate for Ar^{+} dominates and therefore is the source of the HHG emission. if the laser pulse is longer, full ionization of neutrals occurs at even lower laser intensities in the pulse and therefore strengthens the argument for emission from ions. The laser pulse cannot be shorter than 18 fs because of spectral bandwidth limits.

In order to determine the optimum gas pressure to be used when harmonic radiation is generated. Anne L'Huillier [17] have studied in detail how the time- and space-integrated harmonic signal depends on the gas density. They found that at low pressures (a few mbars), the harmonic signal increased approximately quadratically with the pressure, as expected for a coherent process. At pressures of a few tens of mbars the yield saturated, and even decreased with further increase in pressure. The saturation pressure, and the pressure for maximum yield, were found to be order dependent for the high-order harmonics in the cut-off regime. The high harmonic generation in rare gas (Xe, Ar, Ne, He) results from the strong non linear polarization induced by the strong laser field E_{Laser}, at intensity $10^{14} - 10^{15} W/cm^2$.

The process is qualitatively described in the semi-classical three-step model [18]. Close to laser focus, for E_{Laser} comparable to the intra-atomic field, atoms are ionized by tunneling through Coulomb and instantaneous interaction potential (step 1). The ejected electrons are then accelerated by the laser field and gain kinetic energy (step 2). When laser field changes its sign the electron is driven back close to the core and may recombine with atom moving into the ground state, emitting a burst of XUV photons (step 3). This three step process (discussed in next section) repeats every half optical cycle.

High-order harmonic generation in gases (HHG) is now recognized as a very useful source in the XUV range, typically from 100 to 10 nm but even down to the water

window at 3 nm. HHG is relatively easy to produce under conditions of ultra-short pulses ($t \approx 100fs$) of intermediate intensity ($I \approx 10^{15}Wcm^{-2}$) . Harmonic light gets most of its unique characteristics from the fact that HHG is a coherent process tightly driven by the laser field. In addition to the ultra-short pulse duration and high repetition rate, the temporal and spatial coherence [9], regular wave front, or mutual coherence of two harmonic sources originate in the corresponding properties of the driving laser.

The interaction of a strong laser pulse with field strength near the atomic field strength radically differs from light matter interaction at lower intensities so at high laser intensity new type of experiments became possible. Rather than averaging the effect of the integration over many optical cycles as in conventional optics, the electric field can take direct control of electronic motion and imprint its time structure on electron momentum and position. Ionization plays an important role for the precise timing of electronic motion in the field because of its strong non linearity. In most of the cases, the interaction can be described in dipole approximation, i.e. we can neglect spatial variations of the field can be neglected. This is because the extension of the interaction system is, in general, much smaller than wave length of the laser i.e. the wave length of the laser field is assumed to be much larger than the atom of Bohr radius $a_0 = 1au$.

Since low wavelength laser light are produced which become comparable to atomic size and dipole approximation is no more valid, during laser-matter interaction. Even magnetic field component produced by high intensity laser can not be neglected. This magnetic field induces a drift in the laser propagation direction that, for a free classical electron can be quite large and it can inhibit the recombination step. This is not taken in account within the dipole approximation. The magnetic field can influence and even can be used to enhance HHG. As one moves beyond dipole approximation [19–23] regime, symmetry of time dependent Hamiltonian breaks down and all harmonics i.e.

even and odd both become allowed. It will be interesting to explore the dynamical symmetry rule beyond dipole approximation during the laser matter interaction.

1.3 Three Step Model (Ionization, Propagation And Recombination)

High Harmonic Generation is a quantum mechanical process. It is, however, extremely useful to have worked through the classical problem of a charged particle in an electromagnetic field before dealing with the full complexity of HHG. This semi classical treatment is referred to as the three step Model [18].

Their original theory combines both classical and quantum mechanical elements, first, the tunneling of the electron out from the nucleus through the modified by the slowly oscillating laser field Coulomb barrier was described using the standard theory [24] of tunneling ionization. The electron initial velocity was assumed to be zero following its tunneling out from the nucleus. It should be mentioned that recently the "initial conditions" of electrons ionized by a linearly polarized, high intensity laser field were measured by McNaught [25]. It was found that the initial electron kinetic energy is limited to 0.5 percent of pondermotive energy (U_P) (which is in a good agreement with the assumptions of quasi-static tunneling). The subsequent oscillatory motion of the electron in the laser field, during which the influence of the Coulombic interaction is practically negligible, was described by using classical mechanics. Finally, the recombination of the electron back to the ground state was calculated using the classical cross section for the collision and the quantum mechanically recombination probability. Thus a photon of energy $I_p + E_k$ (E_k is the electrons kinetic energy acquired during the oscillatory motion in the field) is emitted.

Highest photon energy that can be produced from HHG occurs when an electron

is ionized at a phase of 17 degree just after the peak of laser cycle. So the maximum return energy of electron is equals to $3.17U_p$, this number 3.17 comes from the position when electron ionizes with highest energy i.e. at 17 degree just after the peak of laser cycle, as electron can ionize at any point but we are interested only those ionization which re strikes with parent with maximum energy which happens at 17 degree just after the peak of laser cycle. This number 3.17 comes out to zero when electron ionizes at the peak of laser pulse, this is why when electron ionizes at peak it comes with no energy and give no harmonics which is undesirable.

Therefore the maximum attainable energy (cutoff energy) of photon is,

$$E_{max} = I_P + 3.2U_P, \tag{1.1}$$

where I_P is ionization potential, and U_P is ponderomotive energy, which is as follows,

$$U_P = \frac{e^2E^2}{4m\omega^2}, \tag{1.2}$$

where all the symbols have their usual meanings.

In the first step (ionization) of the model, High electric field of laser ionizes electron by tunneling. The external field produced by laser is as strong as the field exerted by the nuclei on the core electron (see Fig. 1.1(b)). In the second step (propagation) of model electron begins to oscillates in laser field, typically 0.5 fs to 1.6 fs for laser at wavelength equals to 800 nm. During the oscillation electron gains kinetic energy (see Fig. 1.1(c)). In the third and final step (recombination) of model, electron re-collide with parent ion and recombine giving up 10 eV to 500 eV energy photon (see Fig. 1.1(d)).

The classical motion of electron in the second step of the IPR model is driven by Newton's second law of motion,

$$F = ma, \tag{1.3}$$

and under the influence of laser field the equation become,

$$eE_0 cos(\omega t + \phi) = m\frac{dv}{dt}. \tag{1.4}$$

where e is electronic charge, E_0 and ω is amplitude and frequency of laser field. After integration of Eq. (1.4) we get,

$$v = \frac{eE_0}{m\omega} sin(\omega t + \phi). \tag{1.5}$$

The pondermotive energy, which is a time average of kinetic energy (K.E.), can be calculated as follows,

$$U_p = [K.E.]_{\text{timeavg.}} = \frac{1}{T}\int_0^T \frac{1}{2}mv^2 dt. \tag{1.6}$$

putting the value of v from Eq. (1.5) we get,

$$U_p = \frac{m}{2T}\int_0^T \frac{e^2E_0^2}{m^2\omega^2} sin^2(\omega t + \phi)dt. \tag{1.7}$$

After interaction, expression for ponder motive energy becomes as follows,

$$U_p = \frac{e^2E_0^2}{4m\omega^2}. \tag{1.8}$$

Using Eq. (1.5) we can write,

$$\frac{dx}{dt} = \frac{eE_0}{m\omega} sin(\omega t + \phi) \tag{1.9}$$

Position of electron is given as,

$$[x]_{x_i}^{x_f} = \left[\frac{-eE_0}{m\omega^2} cos(\omega t + \phi)\right]_{t_i}^{t_f} \tag{1.10}$$

In the last step of IPR model, energy emitted as HHG will be given by kinetic energy of the electron at the time of return $x(t_f) = 0$. This electron tunnels in step 1, at time t_i i.e. $x(t_i) = 0$. One can follow the dynamics of electron ionized at different time and and calculate at what time the electron comes back with how much kinetic

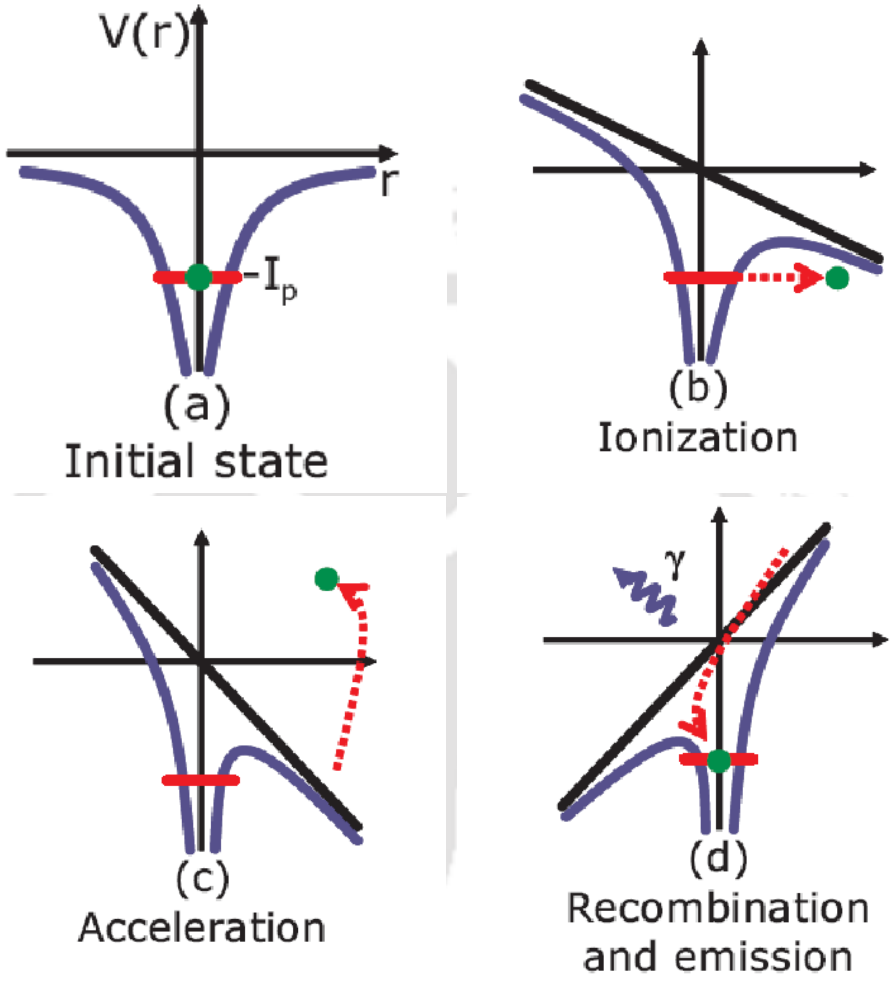

Figure 1.1: (a) Laser is not switched on and electron is under nuclear force only. (b) Laser is switched on and electron goes away from the nuclei in the first half cycle of laser pulse. (c) Electron returns back towards the nuclei in the second half cycle of laser pulse when the pulse changes its sign. (d) Electron recombine with parent ion and produces HHG

energy. The electron released at about 17 degree just after the peak of the field gains maximum kinetic energy at the time of return and that specify the position of cut off i.e. of most energetic harmonics generated.

Harmonic radiation must be generated by atomic electron in the vicinity of nucleus since free electron only oscillates at driving laser frequency. However harmonic radiation is only observed under condition in which substantial above threshold ionization (ATI) also occur. ATI usually compete with the HHG process.

Atoms and molecules with an ionization potential above 10 eV require a laser intensity of the order $10^{14}W/cm^2$ to tunnel through Coulomb barrier (the first step in the three-step model). The maximum tunneling occurs in the vicinity of electric field maxima during the optical cycle. After tunnel ionization at $10^{14}W/cm^2$ depending on the optical phase during which tunneling has occurred, the excited electron may move more than $30\mathring{A}$ away from its parent ion (assuming an 800-nm laser) before being redirected by the laser field (the second step) toward the nuclei.

1.4 High Harmonic Generation Beyond Dipole Approximation

Dipole approximation has been assumed valid in earlier works on HHG. However it is known that as we move to x-ray wavelengths this approximation looses its validity for outer shell electron, and in fact for every wavelength extremely high intensity radiation will bring non dipole Hamiltonian terms into play. Laser matter interaction beyond dipole approximation [19–23], has got its due attention in recent years only. At such intensities electrons may oscillates over a wide range of space and dipole approximation is not going to be valid because during HHG low wavelength laser light is produced which become comparable to atomic size. In the total Hamiltonian

$H = H^0 + H'$ where H^0 is field free Hamiltonian and H' is a interaction term which is given by $H' = \mu.E_0 \cos(\omega t - kz)$. the dipole interaction term remains non-zero over the order of atomic size, but wavelength is order of thousands of $\mathring{A}$. Here k is propagation vector and ω is photon energy. The kz term in H' is ignored. This approximation is called dipole approximation. But at the large intensities this term should not be ignored and it is termed as beyond dipole approximation. Even magnetic field component produced by high intense laser can not be neglected. This magnetic field induces a drift in the laser propagation direction that, for a free classical electron can be quite large and it can inhibit the recombination step of the three step model. This is not taken in account within the dipole approximation. As one move beyond dipole approximation regime, symmetry breaks down and explore all harmonics i.e. even and odd both become allowed.

1.5 Optimization of harmonics using genetic algorithm

Advances in theoretical understanding and experimental techniques has stimulated many studies of optimization and control of High Harmonics depending on various parameters of the laser. In spite of many advantages of HHG, unfortunately a single attosecond pulse generated from high harmonic generation has a low intensity owing to its conversion efficiency, which greatly limits the application of the attosecond pulses. This is because, during HHG the laser pulse creates a free electron density profile, where the largest free electron density is at the pulse peak and the free electron density goes to zero at the pulse backstage. Such a profile gives rise to defocusing, which reduces the laser pulse intensity, which limits the effective interaction length

over which a particular harmonic can be generated. Second reason for this low conversion is, different phase velocities of the fundamental and of the harmonic beam result in a phase mismatch. To modify this situation, femtosecond coherent control with genetic algorithm (GA, which is a modern computer technique) optimization give an impressive method. GA is based on natural selection where a string of binary Numbers is generated. This string corresponds to well defined optimization parameters. The string is called chromosomes. For each chromosome fitness function is calculated. Fitness function is value of the function for the optimization parameter corresponding to that chromosome which is being optimized. Based on the fitness function other chromosome (the next generation) are prepared by mutation and crossover etc. Again the fitness function is calculated for this population and generation of population and calculation of fitness is repeated until the best chromosome is found.

1.6 Application

HHG has various application some of the novel applications are as follows: It provide a source of coherent XUV radiation, suggesting their application in atomic physics such as Soft x-ray interferometry, Point-diffraction interferometry, Ultra-fast atomic and molecular dynamics. For instance Balcou and H. Rabitz [26]measured the relative photo ionization cross section for the rare gases over the range of 10 to 110 eV, using the 11^{th} to 69^{th} harmonic of 140fs Cr:LiSAF laser operating at 825 nm. Harmonics have already been used for solid-state spectroscopy [27] and plasma diagnostics [28]. HHG is used for preparation of attosecond [29–31] or subfemtosecond laser pulses [32], enhancement of pulse energy.

Bibliography

[1] J. Seres, E. Seres, A. J. Verhoef, G. Tempea, C. Streli, P. Wobrauschek, V. Yakovlev, A. Scrinzi, C. Spielmann, and F. Krausz *Nature*, vol. 433, p. 596, 2005.

[2] E. A. Gibson, A. Paul, N. Wagner, R. Tobey, D. Gaudiosi, S. Backus, I. P. Christov, A. Aquila, E. M. Gullikson, D. T. Attwood, M. M. Murnane, and H. C. Kapteyn *Science*, vol. 302, p. 95, 2003.

[3] J. Zhou, J. Peatross, M. Murnane, H. C. Kapteyn, and I. P. Christov *Phys. Rev. Lett.*, vol. 76, p. 752, 1996.

[4] G. Y. Slepyan, S. A. Maksimenko, V. P. Kalosha, A. V. Gusakov, and J. Hermann *Phys. Rev. A*, vol. 63, p. 053808, 2001.

[5] S. Ramakrishna and T. Seideman *Phys. Rev. Lett.*, vol. 99, p. 113901, 2007.

[6] H. C. Kapteyn, M. M. Murnane, and I. P. Christov *Phys. Today*, vol. 58, p. 39, 2005.

[7] M. Lein, N. Hay, R. Velotta, J. P. Marangos, and P. L. Knight *Phys. Rev. Lett.*, vol. 88, p. 183903, 2002.

[8] O. Cohen, X. Zhang, A. L. Lytle, T. Popmintchev, M. M. Murnane, and H. C. Kapteyn *Phys. Rev. Lett.*, vol. 99, p. 053902, 2007.

[9] R. A. Bartels, A. Paul, H. Green, H. C. Kapteyn, M. M. Murnane, S. Backus, I. P. Christovn, Y. Liu, D. Attwood, and C. Jacobsen *Science*, vol. 297, p. 376, 2002.

[10] P. Balcou, R. Haroutunian, S. Sebban, G. Grillon, A. Rousse, G. Mullot, J. Chambaret, G. Rey, A. Antonetti, D. Hulin, L. Roos, D. Descamps, M. B. Gaarde, A. L?Huillier, E. Constant, E. Mevel, D. von der Linde, A. Orisch, A. Tarasevitch, U. Teubner, D. Klpfel, and W. Theobald *Applied Physics B: Lasers and Optics*, vol. 74, 2002.

[11] A. Paul, R. A. Bartels, R. Tobey, H. Green, S. Weiman, I. P. Christov, M. M. Murnane, H. C. Kapteyn, and S. Backus *Nature*, vol. 421, p. 51, 2003.

[12] A. L. Lytle, X. Henge, P. Arpin, O. Cohen, M. M. Murnane, and H. C. K. Lett. *Phys. Rev. A*, vol. 33, p. 2, 2008.

[13] X. Zhang, A. L. Lytle, M. Murnane, H. C. Kapteyn, and O. Cohen *Proceedings of the 15th international coneference, Pacific Grove,USA*, 2006.

[14] D. Zeidler, A. Staudte, A. B. Bardon, D. M. Villeneuve, R. Dorner, and P. B. Corkum *Phys. Rev. Lett.*, vol. 95, p. 203003, 2005.

[15] X. Chu and S.-I. Chu *Phys. Rev. A*, vol. 64, p. 021403, 2001.

[16] X. Chu and S.-I. Chu *Phys. Rev. A*, vol. 64, p. 021403, 2001.

[17] A. L'Huillier *Europhysics News*, vol. 33, p. 6, 2002.

[18] P. B. Corkum *Phys. Rev. Lett.*, vol. 71, p. 1994, 1993.

[19] A. D. Bandrauk and H. Z. Lu *Phys. Rev. A*, vol. 73, p. 013412, 2006.

[20] M. Klaiber, K. Z. Hatsagortsyan, and C. H. Keitel *Phys. Rev. A*, vol. 71, p. 033408, 2005.

[21] T. Kreibich, M. Lein, V. Engel, and E. K. U. Gross *Phys. Rev. Lett.*, vol. 87, p. 103901, 2001.

[22] A. D. Bandrauk, O. F. Kalman, and T. T. N. Dang *J.Chem.Phys.*, vol. 84, p. 12, 1986.

[23] M. Forre, S. Selsto, J. P. Hansen, T. K. Kjeldsen, and L. B. Madsen *Phys. Rev. A*, vol. 76, p. 033415, 2007.

[24] N. B. Delon and V. P. Krainov *J. Opt. Soc. Am. B*, vol. 8, p. 1207, 1991.

[25] S. J. McNaught, J. P. Knauer, and D. D. Meyerhofer *Phys. Rev Lett.*, vol. 78, p. 626, 1997.

[26] P. Balcou and H. Rabitz *Phys. Rev. Lett.*, vol. 68, p. 1500, 1992.

[27] R. Haight and D. R. Peale *Phys. Rev. Lett.*, vol. 70, p. 3979, 1993.

[28] W. Theobald, Rabner, C. Wulker, and R. Sauerbrey *Phys. Rev. Lett.*, vol. 77, p. 298, 1996.

[29] R. Kien, E. Goulielmakis, M. Uiberacker, A. Baltuska, V. Yakovlev, F. Bammer, A. Scrinzi, T. Westerwalbesloh, U. Kleineberg, U. Heinzmann, M. Drescher, and F. Krausz *Nature*, vol. 427, p. 817, 2004.

[30] P. M. Paul, E. S. Toma, P. Breger, G. Mullot, F. Aug, P. Balcou, H. G. Muller, and P. Agostini *Science*, vol. 292, p. 1689, 2001.

[31] G. Sansone, E. Benedetti, F. Calegari, C. Vozzi, L. Avaldi, R. Flammini, L. Poletto, P. Villoresi, C. Altucci, R. Velotta, S. Stagira, S. D. Silvestri, and M. Nisoli *Science*, vol. 314, p. 443, 2006.

[32] P. H. Bucksbaum *Science*, vol. 312, p. 373, 2006.

Chapter 2

Formulation and methodology

2.1 Floquet theory

Consider following ordinary differential equations,

$$\dot{x} = A(t)x, \tag{2.1}$$

where $A(t)$ is a continuous periodic function with period T. The theory of these equation is known as Floquet theory (named after Gaston Floquet) [1–3]. Consider the time dependent Schrodinger equation,

$$i\hbar\frac{d}{dt}\psi(x,t) = H(x,t)\psi(x,t), \tag{2.2}$$

where the Hamiltonian is periodic in time with period T,

$$H(x,t+T) = H(x,t). \tag{2.3}$$

The Floquet theory states that the solution of periodic time dependent Schrodinger equation can be written as,

$$\psi_\lambda(x,t) = \exp(-i\epsilon_\lambda t/\hbar)\phi_\lambda(x,t) \tag{2.4}$$

where $\phi_\lambda(t) = \phi_\lambda(t+T)$. ϕ_λ are called Floquet states. Putting ψ_λ into Schrodinger equation and rearranging we get,

$$H_f(x,t)\phi_\lambda(x,t) = \epsilon_\lambda \phi_\lambda(x,t) \tag{2.5}$$

where,

$$H_f(x,t) = H(x,t) - i\hbar\frac{\partial}{\partial t} \tag{2.6}$$

This is called Floquet Hamiltonian and $\phi_\lambda(x,t)$ is called a Floquet eigenstate. Above equation (2.5) is an eigen value equation in two variables, (x,t), with time dependent eigenvalues given by the Floquet energies, ϵ_λ also called as quasi energy. The key result of Floquet theory is that the Floquet eigen $\phi_\lambda(x,t)$, are periodic in time with the same period T as the Hamiltonian. General solution of the TDSE can be written as,

$$\psi(x,t) = \sum_\lambda a_\lambda \exp((-i\epsilon_\lambda t/\hbar))\phi_\lambda(x,t). \tag{2.7}$$

If ϕ_λ is known over one optical cycle, the ψ can be calculated after any interval. Equation (2.4) can also be rearranged as follows,

$$\psi_\lambda(x,t) = \exp(-i\epsilon_\lambda t/\hbar)\phi_\lambda(x,t) \tag{2.8}$$

$$\psi_\lambda(x,t) = \exp(-i(\epsilon_\lambda + n\hbar\omega)t/\hbar)\exp(in\omega t)\phi_\lambda(x,t) \tag{2.9}$$

This rearrangement corresponds to a series of new Floquet eigenvalue, $\epsilon_\lambda + n\hbar\omega$ with corresponding eigenfunctions,

$$\phi_{\lambda n}(x,t) = \exp(in\omega t)\phi_\lambda(x,t). \tag{2.10}$$

If n is an integer $\phi_{\lambda n}(x,t)$ will be periodic in t so long as $\psi_\lambda(x,t)$ is. Still the physical state $\phi_\lambda(x,t)$ is unchanged, and thus the Floquet eigenvalues associated with distinct physical state are defined only within the range of 0 to $|\hbar\omega|$.

2.2 Dynamical Symmetry Rules

Numerous experimental [4–6] and theoretical investigations of high harmonic generation have shown that noble gases in intense linearly polarized laser light produces odd harmonics but with intense circularly polarized laser light produces no harmonics. This can be explained by dynamical symmetry (DS) [7]. It has been shown that HHG in He can be treated as a single Floquet state phenomenon [8]. The Floquet vectors are eigen vectors of Floquet Hamiltonian

$$H_f = H_0 + xE\cos(\omega t) - i\hbar\frac{\partial}{\partial t} \tag{2.11}$$

where, H_0 is field free Hamiltonian and E is electric field amplitude polarized in X direction. The Floquet Hamiltonian is invariant under 2nd order dynamical symmetry defined as,

$$P_2 = (x \to -x, t \to t + \tau/2) \tag{2.12}$$

where $\tau = 2\pi/\omega$. Since Floquet vector is eigen function of Floquet Hamiltonian and the Hamiltonian and symmetry operator P_2 commute, then the Floquet vector is eigen function of both the operator simultaneously if there is no degeneracy in the Floquet vectors. The probability to emit the n^{th} harmonic (I^n) is obtained from the Fourier transform of the time-dependent dipole of the system,

$$I^n \propto |\int \langle\phi|x\exp(-in\omega t)|\phi\rangle dt|^2 = |\int \langle P_2^{-1}\phi|P_2 x\exp(-in\omega t)P_2^{-1}|P_2\phi\rangle dt|^2 \tag{2.13}$$

To get nonzero n^{th} harmonic,

$$x\exp(-in\omega t) = P_2 x\exp(-in\omega t)P_2^{-1}, \tag{2.14}$$

should not vanish. By applying P_2 operator i.e. replacing x with -x and t with $t+\tau/2$ we get,

$$P_2 x \exp(-in\omega t) P_2^{-1} = -x \exp(-in\omega(t+\tau/2)). \tag{2.15}$$

the equality holds only for odd n hence only x polarized odd harmonics are produced and no even order harmonics will be generated.

The DS rules can be extended to the case of a DS of an arbitrary order N. In that case non zero harmonics will be obtained if and only if $n = Nm \pm 1$ where m is any arbitrary integer. For the system with C_N symmetry interacting with circularly polarized laser light within dipole approximation the Floquet Hamiltonian is given by,

$$H_f = H_0 + xE_0 cos(\omega t) + yE_0 sin(\omega t) - i\hbar\frac{\partial}{\partial t} \tag{2.16}$$

and the dynamical symmetry operators as,

$$P_N = (x \to xcos(\frac{2\pi}{N}) - ysin(\frac{2\pi}{N}), y \to xsin(\frac{2\pi}{N}) + ycos(\frac{2\pi}{N}), t \to t + \tau/N). \tag{2.17}$$

Applying this P_N operator to the Hamiltonian we get,

$$\begin{aligned} P_N^{-1} H_f P_N = H_0 &+ (xcos(2\pi/N) - ysin(2\pi/N)) E_0 cos(\omega t + \omega\tau/N) \\ &+ (xsin(2\pi/N) + ycos(2\pi/N)) E_0 sin(\omega t + \omega\tau/N) - i\hbar\frac{\partial}{\partial t} \end{aligned} \tag{2.18}$$

solving this simple trigonometry we get,

$$P_N^{-1} H_f P_N = H_0 + xE_0 cos(\omega t) + yE_0 sin(\omega t) - i\hbar\frac{\partial}{\partial t} = H_f \tag{2.19}$$

So we observe here that H_f is invariant under P_N .

To get nonzero n^{th} harmonic the integral in Eq. (1.88) under P_N dynamical symmetry,

$$x \exp(-in\omega t) = P_N x \exp(-in\omega t) P_N^{-1}, \tag{2.20}$$

should not vanish. By applying P_N we get,

$$P_N x \exp(-in\omega t) P_N^{-1} = -x \exp(-in\omega(t + \tau/N)). \tag{2.21}$$

the equality holds only for $mN \pm 1$ hence only $n = mN \pm 1$ harmonics are produced (where m is a positive integer).

2.3 Tight binding method

Tight binding method [9, 10] is an approximate model, used especially in solid state physics, to study the band structure. It is the simplest model of interacting particle with only term consisting on site and immediate neighbor interactions. These energy terms are calculated using semi-empirical method. To calculate the matrix elements (not listed in literature) we have used the tight binding basis function k_α in terms of p type atomic orbitals such that,

$$k_\alpha = \psi_\alpha(r - R_\alpha) \tag{2.22}$$

where ψ_α is atomic orbital centered at α^{th} carbon.

For the calculation of the matrix elements we have used three type of coordinate systems as shown in figure (2.1). Global coordinate system (x,y,z), atom position dependent local coordinate system $(x_\alpha, y_\alpha, z_\alpha)$ centered on α^{th} carbon, and bond dependent coordinate system $(x_{\beta\gamma}, y_{\beta\gamma}, z_{\beta\gamma})$, where $x_{\beta\gamma}$ is along the bond between β and γ carbon and $y_{\beta\gamma}$ is perpendicular to $x_{\beta\gamma}$ but in the plane of molecule. $z_{\beta\gamma}$ is perpendicular to the plane of molecule. A local coordinate system is attached with each site and the bond dependent coordinate system is attached to each bond. In the case of $(C_2H_2)_n$ each local coordinate is same as the global coordinate system.

In the case of CNT rolled around z axis, global and local z axis remain same. Graphite sheet which after rolling along z direction gives CNT is shown in Fig. (2.2).

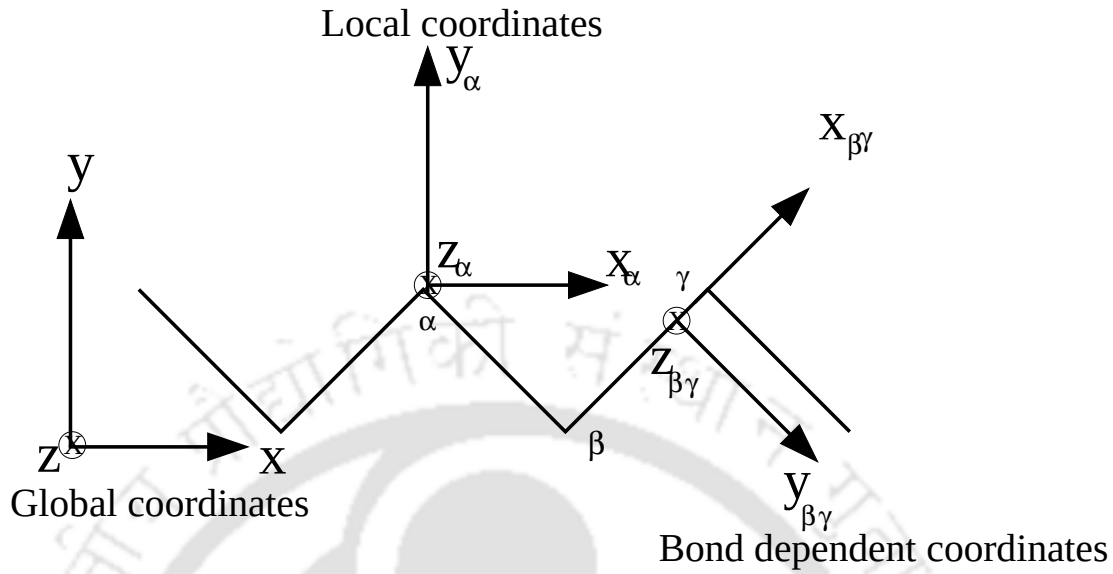

Figure 2.1: Model system of polyacetylene with different coordinate systems.

x axis will be always tangent to the CNT surface and y axis will always be normal to the CNT surface. So local coordinate system will change as the position of carbon atom changes. Bond dependent coordinate system has the same definition as in $(C_2H_2)_n$.

The time dependent Hamiltonian matrix in laser field is given by,

$$H(t) = H^0 + \frac{e}{2mc}\vec{A}.\vec{P} \tag{2.23}$$

where $\vec{A}$ is laser vector potential and $\vec{P}$ is momentum operator, and H^0 is field free Hamiltonian. To perform the calculation one needs matrix elements for H^0 and momentum operators. The matrix elements for H^0 operator in bond dependent coordinate system using semi-empirical method listed in literature [11]. The matrix elements for momentum operators are calculated by performing explicit integration [12].

But to perform our calculation we need to calculate the matrix elements in the

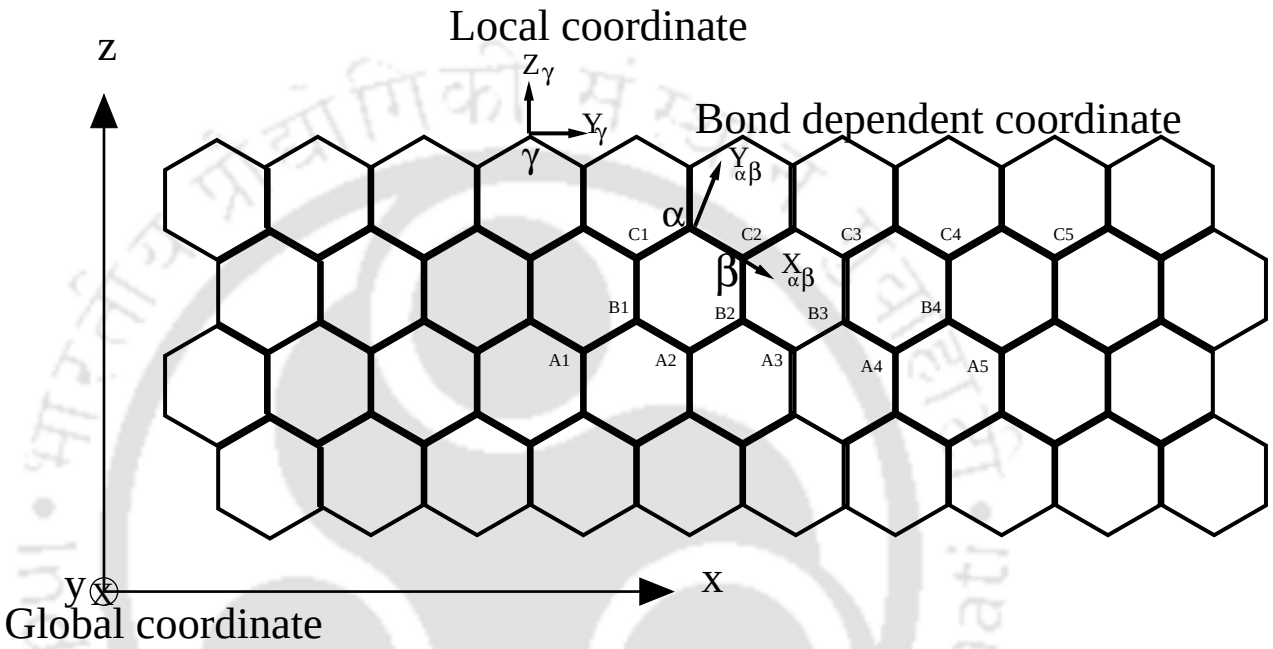

Figure 2.2: Graphite sheet which after rolling along z direction gives CNT. Different coordinate systems are shown. Bond dependent coordinate system has same definition as in the case of C_2H_2, global and local z direction is same. x axis in local coordinate system will be tangent to the CNT surface whereas y axis in local coordinate system will be normal to the CNT surface. After rolling, individual local x, y axis will be different from global axises.

basis,

$$\psi_\alpha(\vec{r}-\vec{R}_\alpha) = |2p_{z\alpha}\rangle$$

$$|2p_{z\alpha}\rangle = (\frac{1}{4\pi})^{1/2}(\frac{z_{2p}}{2a_0})^{3/2}(\frac{z_{2p}}{a_0})z\exp(-\frac{z_{2p}}{2}r) \tag{2.24}$$

Here $r = |\vec{r}-\vec{R}_\alpha|$ and (x,y,z) are the Cartesian components of $(\vec{r}-\vec{R}_\alpha)$. The value of effective nuclear charge is $z_{2p} = 1.78$ for $2p$ type orbitals, where we choose to describe the atomic orbitals in the local coordinate system. We employ the tight binding approach where only nearest neighbor interactions are considered, i.e.,

$$\langle\psi_\alpha(\vec{r}-\vec{R}_\alpha)|H|\psi_\beta(\vec{r}-\vec{R}_\beta)\rangle = 0 \quad \text{if } \alpha \text{ and } \beta \text{ are not neighbors,}$$

where neighbors are carbon atoms which are connected by a chemical bond. The fact that $\langle\psi_\alpha(\vec{r}-\vec{R}_\alpha)|p|\psi_{\alpha+2}(\vec{r}-\vec{R}_{\alpha+2})\rangle$ is sometimes smaller even by one order than $\langle\psi_\alpha(\vec{r}-\vec{R}_\alpha)|p|\psi_{\alpha+1}(\vec{r}-\vec{R}_{\alpha+1})\rangle$ justifies our use of the tight binding model. The matrix elements can be divided into two category, $H_{\alpha\alpha}$ type and $H_{\alpha\beta}$ type where α and β are neighbors and all other elements are zero. In the first category, the Hamiltonian matrix elements are,

$$H_{\alpha,\alpha} = \langle\psi_\alpha(\vec{r}-\vec{R}_\alpha)|H|\psi_\alpha(\vec{r}-\vec{R}_\alpha)\rangle = \epsilon, \tag{2.25}$$

where $\epsilon = 0$, which defines the reference and the momentum matrix elements $P_{\alpha\alpha}$ are all zero due to the symmetry.

In the second category, the matrix elements are calculated when the basis set is described in bond dependent coordinate system as shown in Fig. (2.3) (see the caption).

In our problem we have described the atomic orbitals in local dependent coordinates. Hence we need to resolve the atomic orbitals expressed in local dependent

Figure 2.3: The Hamiltonian and momentum matrix elements for atomic orbitals, when the orbitals are described in bond dependent coordinate system. But in our problem, we choose to describe the atomic orbitals in local dependent coordinates. Hence we need to project the atomic orbitals expressed in local dependent coordinates into orbitals expressed in bond dependent coordinates. The different matrix elements are as follows, $\langle p_{x_{\alpha\beta}}(\beta)|H|p_{y_{\alpha\beta}}(\alpha)\rangle = H_\pi$, $\langle p_{y_{\alpha\beta}}(\beta)|P_{x_{\alpha\beta}}|p_{y_{\alpha\beta}}(\alpha)\rangle = P_{x,\pi}$, $\langle p_{y_{\alpha\beta}}(\beta)|P_{y_{\alpha\beta}}|p_{y_{\alpha\beta}}(\alpha)\rangle = 0$. The values of H_π, s_π, and p_π are -0.1115, 0.129 and (0,0.206) respectively.

coordinates into orbitals expressed in bond dependent coordinates. After the resolution (for C_2H_2) in bond dependent coordinate and rotating the momentum matrix elements in global coordinate system, matrix elements are,

$$\langle p_{z_\alpha}(\alpha)|P_x|p_{z_\beta}(\beta)\rangle = P_{x\pi}cos\pi/6$$

,

$$\langle p_{z_\alpha}(\alpha)|P_y|p_{z_\beta}(\beta)\rangle = -P_{x\pi}sin\pi/6$$

.

In case of CNT, the angle of individual bond dependent coordinate system w.r.t. global coordinate system is calculated. And the matrix elements calculated in bond dependent coordinate system are rotated into global coordinate system.

2.4 Formulation

When a spatially uniform and temporally periodic electric field is applied to the system the time dependent Schrodinger equation (in a.u.) will be,

$$\frac{\partial\psi}{\partial t} = -i\left[\hat{\mathcal{H}}^0 - \frac{e}{mc}\hat{\vec{p}}.\vec{A}(t,x) + \frac{e^2}{2mc^2}A^2\right]\psi \tag{2.26}$$

where,

$$\hat{\mathcal{H}}^0 = \hat{p}^2/2m + v(r), \tag{2.27}$$

is field free Hamiltonian and m, e and $\vec{p}$ are mass, charge and momentum operator of the electron respectively. $\vec{A}$ is the vector potential given by,

$$\vec{A} = (0, A_0\cos(\omega t - kx), A_0\sin(\omega t - kx)). \tag{2.28}$$

The laser field is propagating in x direction (along the axis of system) and polarized in z plane. In the other extreme case of light propagating perpendicular to the axis of the

system, no beyond dipole contribution to the HHG will be present. This particular arrangement has been chosen to maximize the BDA effect. Since we want the even order harmonics generation due to BDA only, and isolate the generation of even order harmonics from any other mechanism, we have used CW laser in the simulation (as a short pulse will also produce even order harmonics). Usually the wavelength of the applied field is much greater than the dimension of the system. So the vector potential can be approximated as,

$$\vec{A} = (0, A_0 \cos(\omega t), A_0 \sin(\omega t)).$$

This is known as dipole approximation. When no such approximation is made then it is termed as beyond dipole approximation. The vector potential is related to the electric and magnetic field as,

$$\vec{E}(r,t) = -\frac{1}{c}\frac{\partial \vec{A}(r,t)}{\partial t}, \tag{2.29}$$

and

$$\vec{B}(r,t) = \vec{\nabla} \times \vec{A}(r,t). \tag{2.30}$$

Within DA, magnetic field ($\vec{B}$) becomes zero, as spatial dependence in $\vec{A}$ is ignored while in BDA regime the effect of magnetic interaction is taken into account.

We have used a tight binding basis set. In the Eq. (2.16), wave function,

$$\psi = \sum c_i(t) p_{z_i}(r), \tag{2.31}$$

is substituted, where p_{z_i} is $2p_z$ type orbital centered on the i^{th} carbon. Multiplying both side by p_{z_j} and integrating over whole space we get,

$$\sum_i \frac{\partial c_i}{\partial t} s_{ji} = -i \sum_i \left[\hat{\mathcal{H}^0_{ji}} + \frac{e}{mc} \langle p_{z_j} | \hat{\vec{p}}.\vec{A} | p_{z_i} \rangle - \frac{e^2}{2mc^2} \langle p_{z_j} | A^2 | p_{z_i} \rangle \right] c_i, \tag{2.32}$$

where s_{ij} and $\mathcal{H}^0_{ij}$ are overlap and Hamiltonian matrix element. In this model, only interaction with the nearest neighbor's has been included. As the orbitals are localized

function, the vector potential can be considered as constant around the region of neighboring atoms. So integrals involving the vector potential are approximated as,

$$\langle p_{z_j}|\hat{\vec{p}}.\vec{A}|p_{z_i}\rangle = \langle p_{z_j}|\hat{\vec{p}}|p_{z_i}\rangle.\vec{A}\left(t, \frac{z_i + z_j}{2}\right), \tag{2.33}$$

and,

$$\langle p_{z_j}|A^2|p_{z_i}\rangle = \left[A\left(t, \frac{z_i + z_j}{2}\right)\right]^2 s_{ji}. \tag{2.34}$$

Using Floquet theorem the solution of the time dependent Schrodinger equation can be written as,

$$\psi(t) = \exp\left(-i\epsilon^{QE}t\right)\phi(t), \tag{2.35}$$

where, $\phi(t)$ is a time periodic functions. ϵ^{QE} and ϕ are the corresponding eigenvalue (quasi-energy) and eigenfunction (Floquet state) of the Floquet Hamiltonian,

$$\hat{\mathcal{H}}_f(t)\phi(t) = \epsilon^{QE}\phi(t). \tag{2.36}$$

The probability to emit the n^{th} harmonic (I^n) is obtained from the Fourier transform of the time-dependent momentum of the system,

$$I^n \propto \left|\int_0^\infty \exp(-in\omega t)p(t).dt\right|^2, \tag{2.37}$$

where the time-dependent momentum is defined as,

$$p(t) = \langle\phi(r,t)|\hat{p}_y|\phi(r,t)\rangle, \tag{2.38}$$

and $n\omega$ is the n^{th} emitted harmonics frequency.

Within DA, due to dynamical symmetry we must get only odd order harmonics and intensity of side band and even harmonics will be zero. But we expect to get both (even as well as odd) harmonics in the case of BDA. Depending upon the extent

of breakdown of DA, its validity can be checked by observing the intensity of dipole forbidden even harmonics.

Spectral entropy (S) of the system is defined as,

$$S = -\sum |p_i| log(|p_i|), \tag{2.39}$$

where p_i' is the time-dependent population of the i^{th} molecular orbital (MO).

Bibliography

[1] G. Floquet *Anne. de l'Ecole Norm. Suppl.*, vol. 12, p. 47, 1983.

[2] H. Sambe *Phys. Rev. A*, vol. 7, p. 2203, 1973.

[3] J. Howland *Math. Ann.*, vol. 207, p. 315, 1974.

[4] A. McPherson, G. Gibson, H. Jara, U. Johann, T. S. Luk, I. A. McIntyre, K. Boyer, and C. K. Rhodes *J. Opt. Soc. Am. B*, vol. 4, p. 595, 1987.

[5] X. F. Li, A. L'Huillier, M. Ferray, L. A. Lompre, and G. Mainfray *Phys. Rev. A*, vol. 39, p. 5751, 1989.

[6] M. Ferray, A. L'Huillier, X. F. Li, L. A. Lompre, G. Mainfray, and C. Manus *J. Phys. B: At. Mol. Opt. Phys.*, vol. 21, p. L31, 1988.

[7] O. E. Alon, V. Averbukh, and N. Moiseyev *Phys. Rev. Lett.*, vol. 80, p. 3743, 1998.

[8] N. Moiseyev and F. Weinhold *Phys. Rev. Lett.*, vol. 78, p. 2100, 1997.

[9] C.-Z. Wang, W.-C. Lu, Y.-X. Y. J. Li, S. Yip, and K.-M. Ho *Sci Model Simul*, vol. 15, p. 81, 2008.

[10] A. Altland and B. Simons, *Interaction effects in tight-binding system*. Cambridge University press, 2006.

[11] R. Saito, G. Dresselhaus, and M. S. Dresselhaus, *Physical properties of carbon nanotubes*. London: Imperial college press, 1998.

[12] A. K. Gupta, O. E. Alon, and N. Moiseyev *Phys. Rev. B*, vol. 68, p. 205101, 2003.

Chapter 3

Even Order Harmonic Generation due to Beyond Dipole Approximation

3.1 Abstract

We have presented here a study of high harmonic generation with model system of polyacetylene irradiated with intense, linearly polarized (perpendicular to the system axis) laser field propagating along the system axis. Only odd order harmonics will be produced within dipole approximation due to dynamical symmetry of the system but all harmonics (odd as well as even order) are expected in the case of beyond dipole approximation. The validity of dipole approximation is studied as a function of number of monomer units in the system which can be quantified by comparing intensity, of even harmonics to odd harmonics. The intensity difference between odd harmonics and even harmonics is strongly dependent on number of monomer unit of ethylene taken and the intensity of applied laser field e.g. in case of high intensity of

laser field and higher number of monomer units of ethylene, even harmonics become more intense than odd harmonics. It is observed that even if electron oscillation is confined to a small region, non dipole term can not be ignored.

3.2 Introduction

In the step two of the semi classical model as discussed in chapter 1, the electron can oscillate over large distances at high intensity and non dipole effects [1–8] can not be ignored. It has been observed that non dipole effects modify the above threshold ionization (ATI) process significantly. A very clear evidence of non dipole effects is seen in the differential probability distributions of the emitted photo electron. Till date most of the theoretical and experimental studies on high harmonic generation has focused on the response of atoms, molecules, ions etc within dipole approximation (DA) regime. Beyond DA [9–12], has got its due attention in recent years only. The laser magnetic field induces a drift in the laser propagation direction that, for a free classical electron can be quite large and it can inhibit the recombination step which can lead to a drastic reduction of the efficiency of HHG [11]. This is not taken into account within the dipole approximation.

In this chapter we have tried to examine the validity of dipole approximation as a function of oscillation amplitude of electron. We have chosen a model system whose length can be varied as we add more number of monomers. A tight binding basis set is selected to describe the electronic wave function. The electron is confined over the length of system so that the electron oscillation amplitude can be equated to the length of the system. This system will produce only odd order harmonics within dipole approximation due to dynamical symmetry rule [13, 14] whereas all the harmonics (both even and odd harmonics due to breaking of symmetry) [15] are expected beyond DA. We expect that as the chain length of the model system

increases, contribution from non dipole term will increase hence intensity of even harmonics compared to the odd harmonics will become more pronounced.

3.3 Results and discussion

In Fig. 3.1, HHG spectra is plotted for polyacetylene with different number of monomer units (1, 3, 5, 10 from top to bottom) irradiated with laser of the electric field strength of 0.9 a.u. and frequency of 0.06 a.u., within DA (left column) and beyond DA (right column). The even harmonics in the case of within DA are not seen as their intensity is close to 10^{-30}. As expected, only odd harmonics are produced in the case of within DA, and both even and odd harmonics are produced in the case of beyond DA. Only odd harmonics in the case of within DA are due to dynamical symmetry of the Hamiltonian [13]. No such symmetry exist in the case of beyond DA. In beyond DA case the intensity of odd harmonics is still couple of order higher than even harmonics for single monomer unit of ethylene. This implies that Dipole approximation is just valid when electron can access region equivalent to only single π bond. When HHG is calculated from smaller number of monomer the dipole approximation should be valid. Here p_z orbitals are used as localized basis functions.

It is clearly evident from Fig. 1, that the difference in the intensity of odd order harmonics and even order harmonics in the initial part of the plateau, is comparable when more than single monomer is involved but in the later part of plateau the even harmonics are 3 to 4 order higher in intensity than odd order harmonics. The terminal carbon to carbon distance is approximately $8\mathring{A}$ for polyacetylene with 3 monomers and here surprisingly complete break down of DA occurs.

Another major difference observed is that, as the number of monomers is increased the intensity of harmonic generation in the plateau region within DA, decreases but no appreciable change occur in the case of beyond DA. The plateau cutoff increases

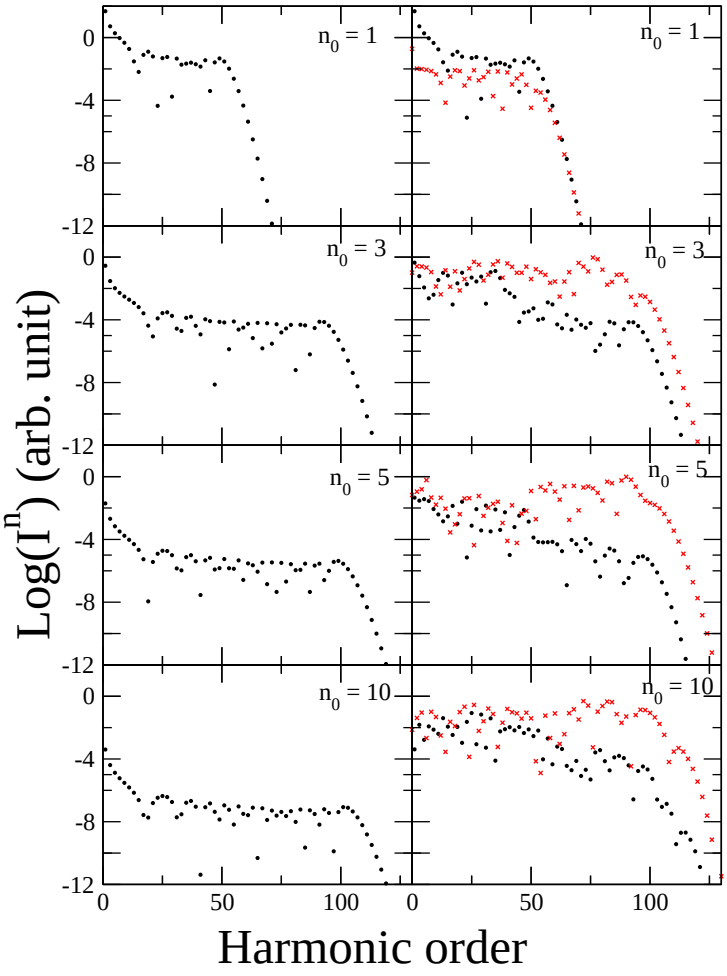

Figure 3.1: HHG spectra of model polyethylene $[H(C_2H_2)_{n_0}H]$ system where π electron is interacting with linearly polarized laser light of electric field strength 0.9 a.u. and frequency 0.06 a.u., within dipole approximation (left) and beyond dipole approximation (right). (dots(*) are the odd harmonics and crosses ($\times$) are the even order harmonics)

in both the cases as a function of number of monomers in similar fashion because of increase in polarizability. Within DA, as the system size increases the energy of orbitals participates through dipole interaction is increasing, hence the polarizability is decreasing. As the system size increases cutoff increases but the intensity of HHG decreases. For this system the plateau cutoff in case of longer chain length, extends up to one hundred and fifty for five number of monomer units which is significantly larger than the plateau in case of only single monomer which extends to around fifty only.

In Fig. 3.2, HHG spectra is plotted as a function of intensity (from top to bottom) for different number of monomer units. For the case of relatively lower intensity of 2 a.u. of linearly polarized laser and only single number of monomer unit of ethylene, the intensity of even harmonics are comparable to odd order harmonics intensity. As the intensity increases even order harmonics become more pronounced and the difference between intensity of even order harmonics and odd order harmonics keeps on getting larger (here the dynamics is extremely complicated and we yet have not studied its reasoning). But in the case of polyacetylene with two monomer units (right), the spectra is much more complicated. In later part of the plateau near the cutoff the even order harmonics is many order intense than odd order harmonics. Close to the cutoff more intense even order harmonics can be generated by increasing number of monomer units of ethylene even if comparatively moderate intensity laser is used. So we can say that for relatively lower laser intensity and lower number of monomer units of ethylene odd order harmonics are of more intensity than even order harmonics (at least for initial range of plateau), and for higher laser intensity and higher number of monomer units of ethylene we get even order harmonics more intense than odd order harmonics for the case of beyond DA.

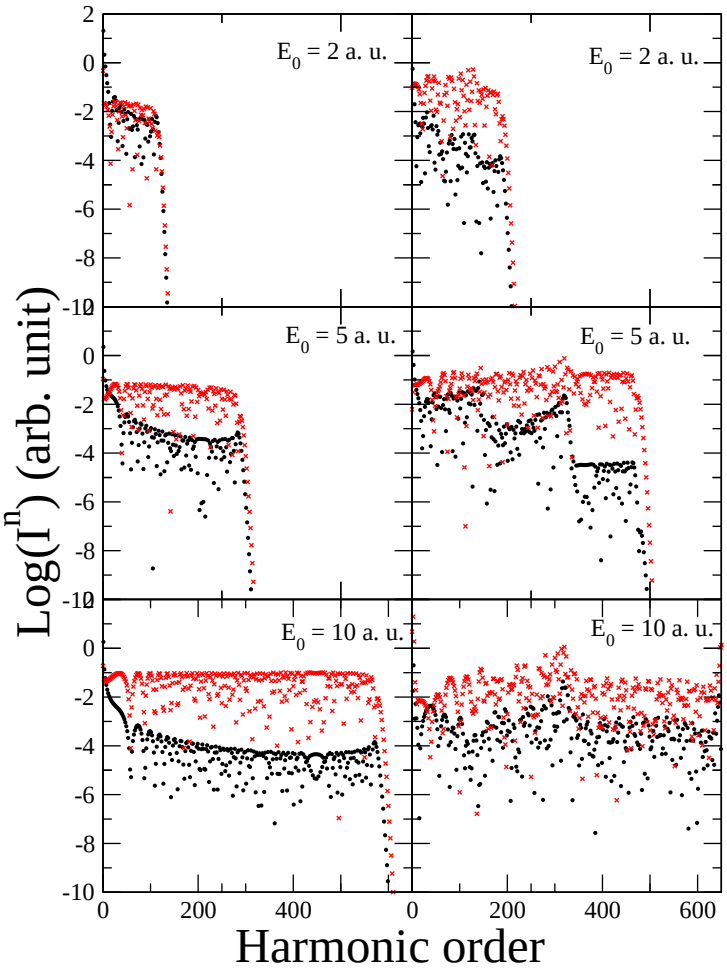

Figure 3.2: HHG spectra from π electron of model system, monomer (left) and dimer (right) of C_2H_2 interacting with linearly polarized laser light. (dots(*) are the odd harmonics and crosses(×) are the even order harmonics)

3.4 Summary

In summary, we have shown that the beyond dipole interaction can fundamentally change the HHG spectra even if electron is confined into a space of $8\mathring{A}$ only during the interaction. The even order harmonics are found to be more intense even if only two monomer units of ethylene are included in model system. With increase in laser intensity the DA become more worse and near the cutoff even harmonics are many order high intense than the odd order harmonics. We conclude that dipole approximation is not valid while solving the time-dependent Schrodinger equation governing the behavior for model polyacetylene system.

Bibliography

[1] M. Forre, J. P. Hansen, L. Kocbach, S. Selsto, and L. B. Madsen *Phys. Rev. Lett.*, vol. 97, p. 043601, 2006.

[2] L. B. Madsen and D. Dimitrovski *Phys. Rev. A*, vol. 78, p. 23403, 2008.

[3] M. Forre, S. Selsto, J. P. Hansen, and L. B. Madsen *Phys. Rev. Lett.*, vol. 95, p. 043601, 2005.

[4] N. J. Kylstra, R. A. Worthington, A. Patel, P. L. Knigh, J. R. V. de Aldana, and L. Roso *Phys. Rev. Lett.*, vol. 85, p. 1835, 2000.

[5] R. E. Wagner, Q. Su, and R. Grobe *Phys. Rev. Lett.*, vol. 84, p. 3282, 2000.

[6] S. X. Hu and C. H. Keitel *Phys. Rev. Lett.*, vol. 83, p. 4709, 1999.

[7] R. Taeb, V. Vniard, and A. Maquet *Phys. Rev. Lett.*, vol. 81, p. 2882, 1998.

[8] S. Patchkovskii, Z. Zhao, T. Brabec, and D. M. Villeneuve1 *Phys. Rev. Lett.*, vol. 97, p. 123003, 2006.

[9] A. D. Bandrauk and H. Z. Lu *Phys. Rev. A*, vol. 73, p. 013412, 2006.

[10] A. D. Bandrauk, O. F. Kalman, and T. T. N. Dang *J.Chem.Phys.*, vol. 84, p. 12, 1986.

[11] M. W. Walser, C. H. Keitel, A. Scrinzi, and T. Brabec *Phys. Rev. Lett.*, vol. 85, p. 5082, 2000.

[12] A. Staudt and C. H. Keitel *J. Phys. B: At. Mol. Opt. Phys.*, vol. 36, p. 203, 2003.

[13] O. E. Alon, V. Averbukh, and N. Moiseyev *Phys. Rev. Lett.*, vol. 80, p. 3743, 1998.

[14] O. E. Alon, V. Averbukh, and N. Moiseyev *Phys. Rev. Lett.*, vol. 85, p. 5218, 2000.

[15] T. Kreibich, M. Lein, V. Engel, and E. K. U. Gross *Phys. Rev. Lett.*, vol. 87, p. 103901, 2001.

Chapter 4

Study of entropy during High Harmonic Generation

4.1 Abstract

We have presented here a study of entropy during high harmonic generation with model system of the polyacetylene irradiated with intense, linearly polarized (perpendicular to the system axis) laser field propagating along the system axis. To investigate the population dynamics of electron in different molecular orbital we have calculated the spectral entropy within dipole approximation and beyond dipole approximation regime during high harmonic generation process. The spectral entropy is a measure of molecular orbital population fluctuation. It is found that there is no change in maximum spectral entropy during the process within dipole approximation as the system chain length increases. But maximum spectral entropy, beyond dipole approximation shows a continuous increases with respect to system chain length. Interestingly HHG plateau increases with laser intensity but has no effect on maximum spectral entropy.

4.2 Introduction

One can use the concept of spectral entropy [1] to explore the molecular orbital population dynamics during the High Harmonic process. Minute changes in population in different molecular orbitals get amplified in the plots of spectral entropy. We get very useful information about the molecular orbitals particularly during the HHG process. Measurement of spectral entropy also allows to check the validity of dipole approximation during laser-matter interaction.

4.3 Results and discussion

In Fig. 4.1, spectral entropy is plotted as a function of time for polyacetylene containing different number of monomer units (1, 2, 3, 4) irradiated with laser of the electric field strength of 0.9 a.u. and frequency of 0.06 a.u., within DA (above) and beyond DA (below). The maximum spectral entropy in the case of within DA remains constant as the number of monomer unit changes in the system. But there is increase in maximum spectral entropy in the case of beyond dipole approximation as the system length increases with increasing more number of monomer units. In Fig. 4.2, we have plotted the HHG spectra for different number of monomer units (1, 2, 3, 4) and it is observed that only odd harmonics are produced in the case of within DA, and both even and odd harmonics are produced in the case of beyond DA. Only odd harmonics in the case of within DA are due to dynamical symmetry of the Hamiltonian [2]. No such symmetry exist in the case of beyond DA. In beyond DA case the intensity of odd harmonics is still couple of order higher than even harmonics for single monomer unit of ethylene. This implies that DA is not valid for laser matter interaction. Here localized p_z orbitals are used as basis functions.

The entropy relates to the fluctuation of population in different MOs. We have

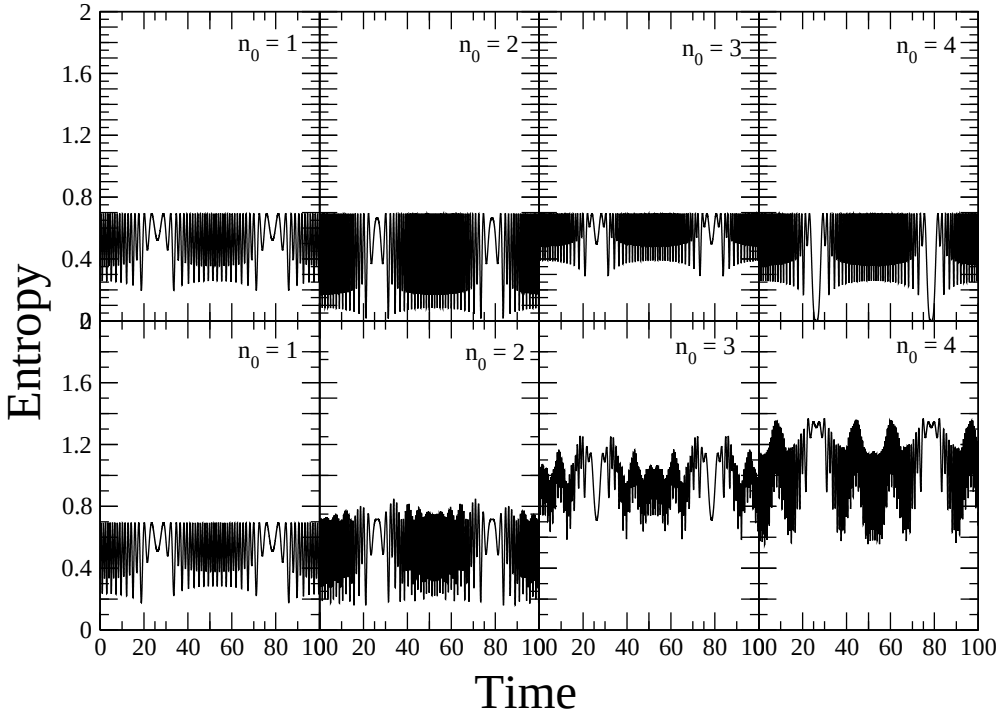

Figure 4.1: Entropy of model polyacetylene $[H(C_2H_2)_{n_0}H]$ system where π electron is interacting with linearly polarized laser light of electric field strength of 0.9 a.u. and frequency 0.06 a.u., within dipole approximation (above) and beyond dipole approximation (below).

plotted the spectral entropy as a function of time for different number of monomer units in the model system. It has been observed that the maximum spectral entropy does not change in the case of within DA but it increases continuously in the case of BDA. In this model system, for ground state molecular orbital non zero transition moment occurs only with the highest molecular orbital. Hence in the case of DA only these two states participate in the dynamics. As the number of units increases, the energy difference between these two states increases and the corresponding transition moment decreases. This leads to the decrease in polarizability. This explains the decrease in the intensity of harmonic generation and increase in plateau cutoff. But in the case of BDA, multipoles will couple all the MOs. Population of dipole forbidden MO is small but significant enough to contribute to the entropy and higher intensity of even order harmonics. As the entropy increases, the intensity corresponding to even order harmonics increases but the odd harmonic intensity remains unchanged.

For example consider the case of C_2H_2. The MOs are shown in Fig. (4.3). In the case of DA, π_1 interacts with π_4^* only and π_2 interact with π_3^* only. But in the case of BDA, in spite of above interaction, π_1 interacts with π_2 and π_3^* also via non dipole effects. Starting from π_1 the π_2^* and π_3^* MOs receives a small but appreciable population, that modify the entropy plots and HHG spectra.

In Fig. 4.4, HHG spectra (above) which is same as in previous chapter to see the changes in the plots of entropy and HHG in same regime and entropy (below) is plotted as a function of intensity (from left to right) for the same number of monomer units. In the case of relatively lower intensity of 2 a.u. of linearly polarized laser light the intensity of even harmonics are comparable to odd order harmonics intensity with some fix entropy. As the intensity increases even order harmonics become more pronounced and the difference between intensity of even order harmonics and odd order harmonics keeps on getting larger at least in the plateau region of HHG spectra. But interestingly there is no change in maximum entropy spectra with respect to the

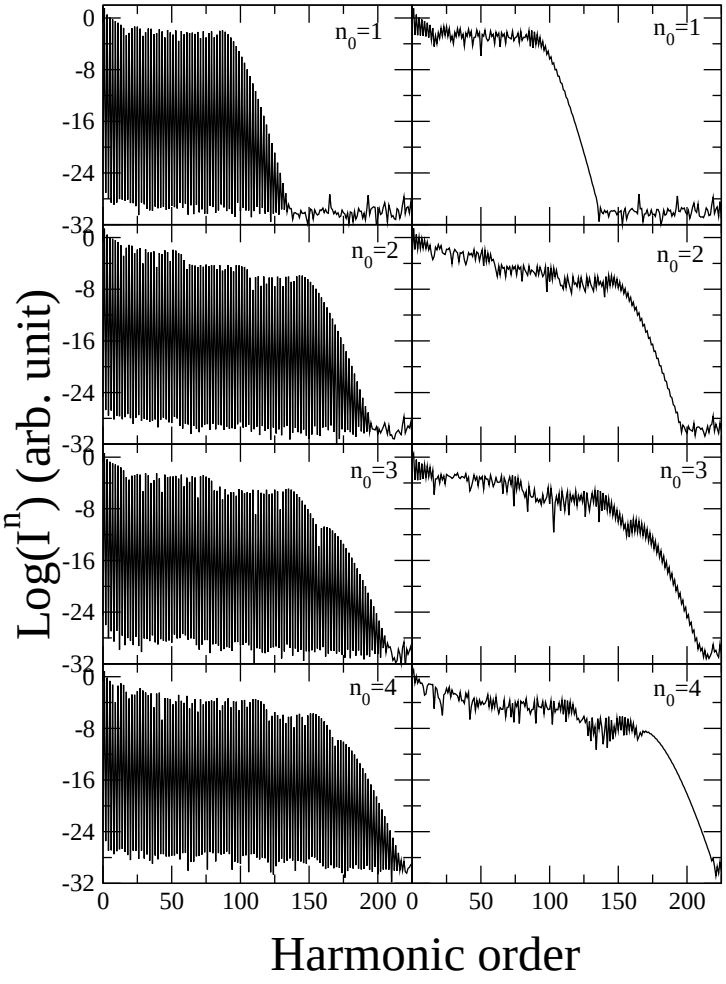

Figure 4.2: HHG spectra of model polyacetylene $[H(C_2H_2)_{n_0}H]$ system where π electron is interacting with linearly polarized laser light of electric field strength of 0.9 a.u. and frequency 0.06 a.u., within dipole approximation (left) and beyond dipole approximation (right).

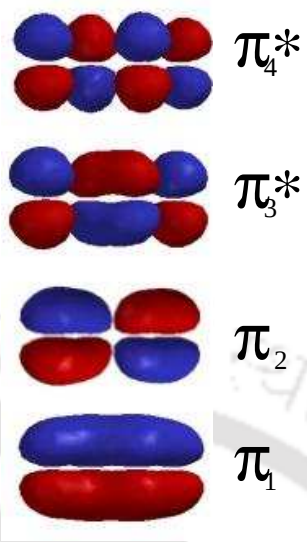

Figure 4.3: Different MO's of $(C_2H_2)_2$ system.

intensity of applied laser field. This comparison reveals that while laser intensity increases the HHG plateau, has no effect on entropy.

4.4 Summary

We have shown that the study of entropy during HHG provides interesting insight about molecular population dynamics. As it is shown that both HHG and entropy spectra changes fundamentally in the case of beyond DA. When all type of the harmonics (even as well as odd) is generated even if electron is confined into a space of $8\mathring{A}$ only during the interaction. We observe the significant increase in entropy in the case of beyond DA regime. These observation strongly support the non validity of DA during the process. So we conclude that dipole approximation is not valid while solving the time-dependent Schrodinger equation governing the behavior for model polyacetylene system.

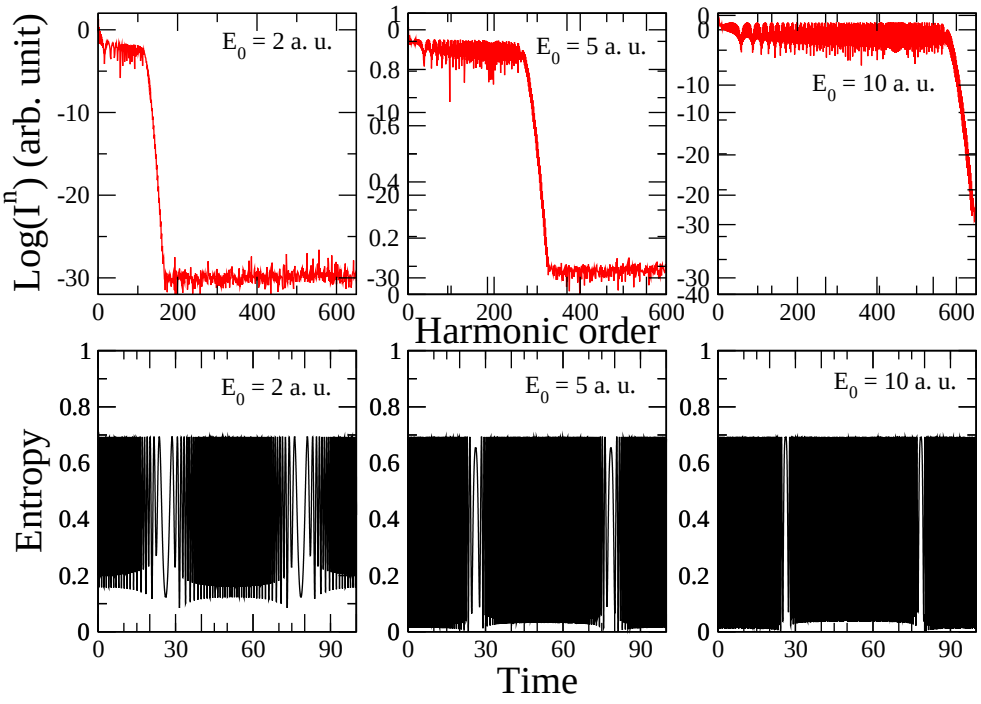

Figure 4.4: Comparison of HHG spectra and Entropy of only monomer unit of model polyacetylene $[H(C_2H_2)_{n_0}H]$ system as a function of laser intensity in the case of beyond dipole approximation.

Bibliography

[1] F. H. M. Faisal and J. Z. Kaminski *Phys. Rev. A*, vol. 56, p. 748, 1997.

[2] O. E. Alon, V. Averbukh, and N. Moiseyev *Phys. Rev. Lett.*, vol. 80, p. 3743, 1998.

Chapter 5

High Harmonic Generation and the validity of Dynamical Symmetry rule for Carbon Nanotube

5.1 Abstract

We present here an investigation of High Harmonics Generation (HHG) from Carbon Nanotube (CNT) using a high intensity CW laser. Here for Linearly polarized (LP) light, due to dynamical symmetry (DS) we should get only allowed harmonics (odd order, when emitted light is polarized in y direction, and even order, when emitted light is polarized in x direction). And in the case of beyond dipole approximation, one should get all the harmonics irrespective of polarization direction of emitted light. Whereas, if a circularly Polaris ed (CP) laser light is used, again due to dynamical symmetry we should get only allowed harmonics [$\Omega = (5n \pm 1)\omega : n = 1, 2, 3.....$, where ω and Ω are the fundamental and harmonic frequencies] in both the cases. We have derived the selection rule for generated light polarized perpendicular to the

incident laser light.

5.2 Introduction

In recent times carbon nano tube has attracted the scientific community a lot because of its various instrumental application. The CNT can be prepared containing different rotational symmetry element. CNT containing C_N [1]symmetry element interacting CP laser light within DA produces $(N \pm 1)^{th}$ harmonic. But with LP laser [2] light it should produce only odd harmonics polarized in the same direction as incoming laser light and even harmonics if polarized perpendicular to incoming laser field vector. In beyond dipole approximation CNT [3] interacting with LP or CP [4] , the selection rules for HHG due to the symmetry of the Hamiltonian breaks down and all the harmonics should be generated. In this paper we have presented the study of the interaction between nanoring and single walled carbon nanotube (SWCNT) with a high intense laser field.

5.3 Classification of CNT

Single walled carbon nanotube (SWCNT) is a result of rolling up of a graphene sheet into a cylinder, which is specified by a chiral vector $C_h = n_1 a_1 + n_2 a_2$ where n_1, n_2 are integers and a_1, a_2 are the elementary vectors of the dimensional graphite lattice. CNTs can be chiral or non chiral, again depending on the way of rolling up. CNTs are classified into three type, namely armchair (n_1, n_1) nanotube, zigzag $(n_1, 0)$ and chiral (n_1, n_2) nanotube with $n_1 \neq n_2$. Zigzag and armchair nanotube are also called achiral. For armchair and zigzag nanotube, when $(n_1 - n_2)$ is divisible by 3, we have conducting tube, otherwise semiconducting nanotube form. For forming metallic CNT, $(2n_1 + n_2)/3$ or equivalently $(n_1 - n_2)/3$ must be an integer. The radius of

CNT is given by $R_{CNT} = \sqrt{3}b\sqrt{n_1^2 + n_2^2 + n_1 n_2}/2\pi$, where $b = 1.42\mathring{A}$ is the distance between the nearest-neighboring carbon atoms in graphite. The physical properties of SWNT is determined by their geometry. Here we have done all our calculations for armchair CNT only.

5.4 Non dipole effects

The ability to generate ultra-short laser pulses delivering intensities over $10^{20}W/cm^2$ allows the study of ultra-fast processes and the investigation of properties of molecules interacting with super intense laser fields. Exciting applications include the development of short wavelength lasers by using high harmonic generation (HHG), strong field interactions with controllable aligned molecules, generation of attosecond pulses, etc. At the core of the laser molecule alignment interaction is the non resonant polarizability that is governed by an induced dipole potential. We have investigated the influence of non-dipole effects on the HHG phenomenon. Super-strong laser fields offer unique possibilities for the investigation of the quantum vacuum.

When we consider the laser with intensities exceeding $10^{15}W/cm^2$, the influence of the magnetic field on electron dynamics becomes non-negligible. Therefore, a theoretical approach beyond the dipole approximation becomes important. Hence, in [5–10] the laser-atom interaction beyond approx. $10^{15}W/cm^2$ has been investigated on the basis of the Schrodinger equation in non dipole approximation.

The evolution of the electron wave-packet in a laser field of arbitrary shape is investigated in [5] in the weakly relativistic regime. The influence of non dipole effects on the stabilization phenomenon in the weakly relativistic regime is investigated for two-electron atoms as well as in the case of excited atomic states [7].

Relativistic effects are especially dramatic for ATI and HHG processes. The laser magnetic field induces a drift of the ionized electron in the laser propagation direction

which severely suppresses the probability of the electron to revisit the ionic core and, consequently, the yield of ATI electrons or harmonic photons. That is why the HHG frequencies cannot be increased by a straightforward increase of the laser intensity.

An interesting possibility to counteract the relativistic drift in the weakly relativistic regime, based on the use of antisymmetric molecular orbitals, is shown in [11]. HHG of a diatomic molecule is investigated by solving the Schrodinger equation numerically, beyond the dipole approximation. Due to symmetry, the momentum distribution of the antisymmetric molecular orbital has two peaks at the nonzero momentum component along the axis of the molecule. Therefore, in a strong laser field the electron tunnels out from the molecule with nonzero momentum along the molecular axis. If the axis is oriented in the laser propagation direction, the initial momentum of the ionized electron will counteract the relativistic drift, allowing for re-scattering and, thus, considerably increasing the harmonic signal.

5.5 Results and discussion

Three main points can be noted here. First the radiation intensity falls off significantly beyond the cutoff. Secondly Beyond the cutoff, there are well-resolved peaks separated by 2ω . And third the spectrum in the plateau does not exhibit harmonic peaks but shows very complicated interference structures. This is because there are more than one electron paths contributing to each harmonic below the cutoff. These degenerate electron paths lead to different time-dependent dipole phases in the dipole moment, which creates a irregular substructures within each harmonic spectrum.

In Fig. 5.1, HHG spectra are plotted for CNT containing different number of unit cells (2, 10, 20) irradiated with linearly polarized laser of the electric field strength of 0.9 a.u. ($2.85 \times 10^{16}\ W/cm^2$) and frequency of 0.06 a.u. (760 nm), in DA regime (above row) and BDA regime (below row). In this case emitted light is polarized in y

direction. As it is shown in Fig. 5.1, there are only even order harmonics in the case of within DA. But in the case of BDA, both even as well odd harmonics are present. The odd harmonic generation are expected due to symmetry requirement and in the case of beyond dipole approximation the symmetry is lost hence inclusion of beyond dipole approximation is important. In Fig. 5.2, x polarized HHG spectra are plotted for the same system and same the parameters in Fig. 5.1, left column of the Fig 5.2, is contain HHG spectra within for DA regime and the right column for BDA regime. As it can be seen that there are only odd order harmonics generated in the case of within DA. But in the case of BDA, both even as well odd harmonics are present. We have shown that emitted light perpendicular to the incident laser polarization can be a source for generation of even order harmonics.

In Fig. 5.3, HHG spectra are plotted for CNT containing different number of unit cells (2, 10, 20) irradiated with circularly polarized laser of the electric field strength of 0.9 a.u. ($2.85 \times 10^{16}\ W/cm^2$) and frequency of 0.06 a.u. (760 nm), Irrespective of emitted light polarization in the case of circularly polarized laser light, we get only allowed $5n \pm 1$ harmonics. And the same is true for the spectra in the DA case too for circularly polarized laser light.

5.6 Summary

In summary, we have shown that in the case of within dipole approximation regime and for linearly polarized laser light, due to dynamical symmetry, x polarized even order harmonics and y polarized odd order harmonics are produced. But in the case of beyond dipole approximation all the harmonics are emitted. When we use circularly polarized laser light is used, in either the case of DA or BDA, due to dynamical symmetry only allowed $5n \pm 1$ harmonics are produced.

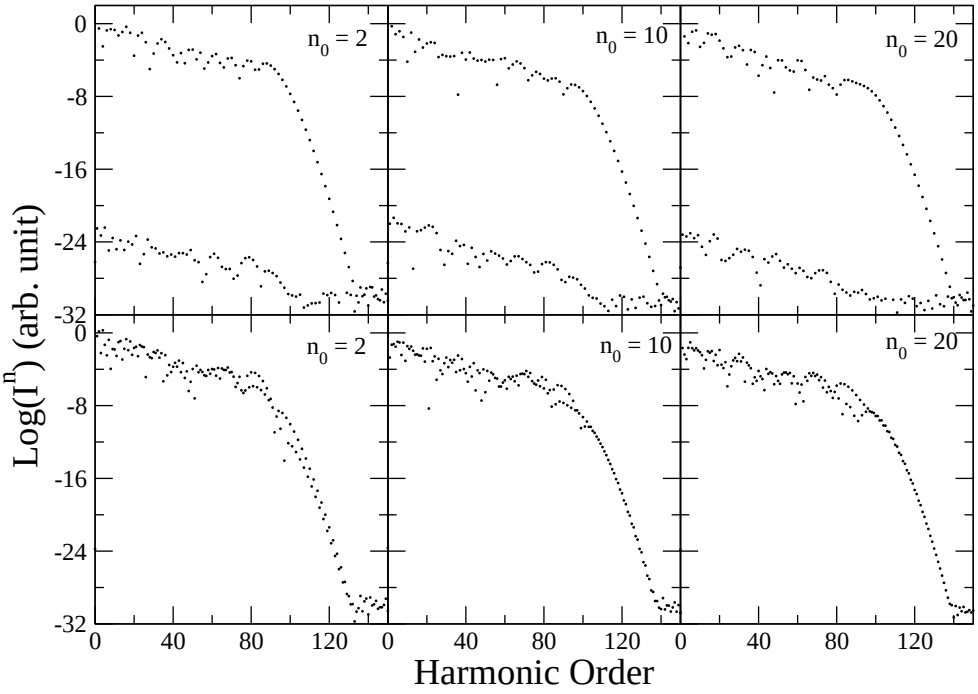

Figure 5.1: y polarized HHG spectra from π electron of model system of CNT containing different (2, 20, 40) number of unit cells interacting with linearly polarized laser light of electric field strength of 0.9 a.u. and frequency 0.06 a.u., within dipole approximation (above) and beyond dipole approximation (below).

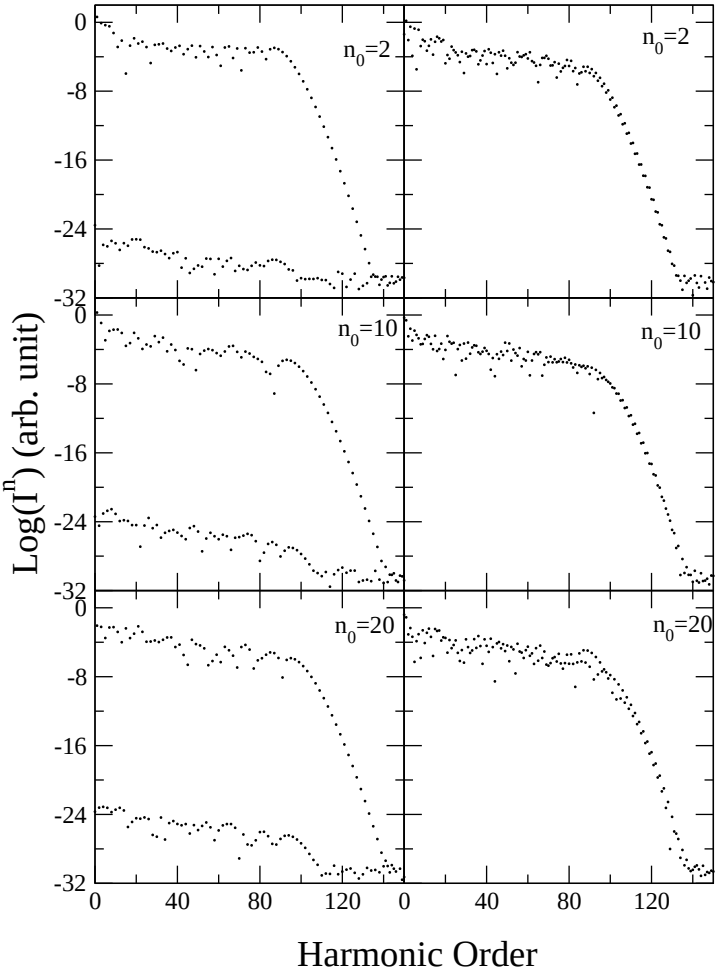

Figure 5.2: x polarized HHG spectra from π electron of model system of CNT containing different (2, 20, 40) number of unit cells interacting with linearly polarized laser light of electric field strength of 0.9 a.u. and frequency 0.06 a.u., within dipole approximation (left) and beyond dipole approximation (right).

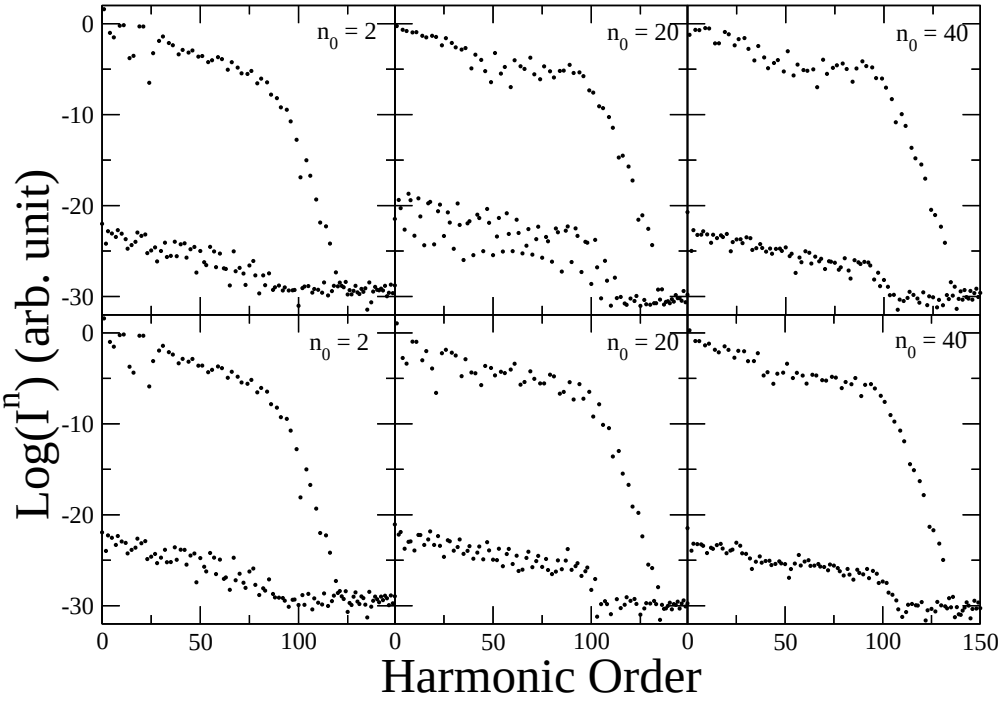

Figure 5.3: HHG spectra from π electron of model system of CNT containing different (2, 20, 40) number of unit cells interacting with circularly polarized laser light of electric field strength of 0.9 a.u. and frequency 0.06 a.u., within dipole approximation (above) and beyond dipole approximation (below).

Bibliography

[1] O. E. Alon, V. Averbukh, and N. Moiseyev *Phys. Rev. Lett.*, vol. 80, p. 3743, 1998.

[2] C. B. Madsen and L. B. Madsen *Phys. Rev. A*, vol. 76, p. 043419, 2007.

[3] G. Y. Slepyan, S. A. Maksimenko, V. P. Kalosha, A. V. Gusakov, and J. Hermann *Phys. Rev. A*, vol. 63, p. 053808, 2001.

[4] A. D. Bandrauk and H. Z. Lu *Phys. Rev. A*, vol. 73, p. 013412, 2006.

[5] M. Verschl and C. H. Keitel *Las. Phys.*, vol. 15, p. 529, 2005.

[6] M. Mahmoudi, Y. I. Salamin, and C. H. Keitel *Phys. Rev. A*, vol. 72, p. 033402, 2005.

[7] A. Staudt and C. H. Keitel *Phys. Rev. A*, vol. 70, p. 043412, 2006.

[8] A. Staudt, C. H. Keitel, and J. S. Briggs *J. Phys. B*, vol. 39, p. 633, 2006.

[9] B. Henrich, K. Z. Hatsagortsyan, and C. H. Keitel *Phys. Rev. Lett.*, vol. 93, p. 013601, 2004.

[10] M. Klaiber, K. Z. Hatsagortsyan, and C. H. Keitel *Phys. Rev. A*, vol. 71, p. 033408, 2005.

[11] R. Fischer, M. Lein, and C. H. Keitel *Phys. Rev. Lett.*, vol. 97, p. 143901, 2006.

Chapter 6

Effect of dipole on harmonic optimization with adaptive control using an evolutionary search process

6.1 abstract

We have presented here a study of optimization of high order harmonic generated in two different case of (a) within dipole approximation and (b) beyond dipole approximation. We have considered model system of ethylene irradiated with intense, linearly polarized (perpendicular to the system axis) laser field propagating along the system axis. It is found that although harmonic intensity increases in both the cases but optimization is always higher in the case of beyond dipole approximation. Study of optimization of even order harmonics as well as odd order harmonics have been done.

6.2 Introduction

In past two decades much efforts have been done to surge up the intensity of harmonics, in order to meet the challenges of attosecond world. As high harmonic generation (HHG) [1–3] has many application including the investigation of molecular orbital shape, preparation of attosecond pulses [4, 5], spectroscopy etc., but in spite of these advantages there are some drawbacks too such as overheating problems in some sensitive instruments, so it become more important to design the harmonics in such a way that one can meet to his requirement accordingly. For this purpose Genetic Algorithm (GA - which is a search tool to find the maximum of multi variable functions resembling closely the biological evolutionary processes.) [6–10] plays a vital role for increasing or suppressing the chosen harmonics [11, 12]. GA has got its due attention in recent years only as many physicist, chemist, computer scientists are using this frequently now a days. Here we will present HHG optimization in the regime of within Dipole Approximation (DA) and Beyond Dipole Approximation (BDA) [13–18] using GA.

Genetic algorithm is based upon the natural selection.Natural selection determines which members of a population survive to reproduce, the species has best chance to continue. To employ the genetic algorithm for engineering design optimization, the parameters of the design are encoded into a string of binary digits. Many strings are randomly chosen. These strings form population and next generation of population is born based upon fitness function. The "fitness" of each string is determined according to required design specifications. GA is based on reproduction, fitness, crossover and mutation. During crossover a random group of nucleotides of two lined up DNA fine threads are changed. Bit strings are known as chromosomes in GA terminology. The process is as follows: select two bit strings (chromosomes), in case of genetic algorithm select a branch of each parent. Cut the chromosomes (or the branch in case of GA)

at a particular location. Swap the bits/branches of the two parents. Crossover can generate a very large amount of different strings. However depending on the initial population chosen, there may not be enough variety in the strings to ensure the GA covers the entire problem space. These problems are overcome by introducing a mutation operator into the GA. The GA has mutation probability, which dictates the frequency at which mutation occurs. Mutation can be performed either during selection or crossover. Mutation depends on the encoding of chromosomes. Since the chromosomes consists of two type of values (amplitude and phase), so two different values were chosen and added, one for the amplitude string and the other for the phase string. Fitness factor (according to Darwin's theory the solution of better fitness has a higher chance to survive) in GA context means assigning a value to one or more strings to get better solution than other strings that result from reproduction, crossover and mutation. The algorithm stops either at a predefined maximum no. of generations or when the accuracy requirement is achieved.

In this chapter, we have investigated the effect of DA on harmonic optimization. The mechanism of the process is qualitatively described by the semi-classical three-step model [19]. Here we have optimized the desired harmonic 51^{st} (i.e. odd order) harmonic in both the case of within DA and beyond DA and surprisingly it is found that consideration of dipole effects [20–27] improves harmonic intensity significantly as compared to the case of without dipole consideration. The amplitudes and phase of the lasers are used as optimization parameters. Only amplitude optimization results are shown. It has been shown that with two colour laser optimization, harmonics intensities are enhanced by order of magnitude. It is observed that optimization [28] is better in the case of beyond DA than the case of within DA. A few experimental studies have been carried out where the optimization are achieved up to a maximum of 17 times [6,9,10]. Even fewer theoretical studies have been attempted to maximize HHG [7, 8] and have not obtained as good as optimization as in the experimental

optimization. All the theoretical studies have been done so far is within DA. It has also been shown that optimization depends on laser pulse durations [29].

6.3 Results and discussion

We have optimized the 51^{th} harmonic in the case of DA and BDA. We have used the intensities of lasers as the parameter for optimization. Amplitude is varied in such a way that total energy of CW pulse within a optical cycle remains same. Maximum allowed value for the amplitude is 0.9 a.u. if amplitude of one pulse is 0.9 a.u. the amplitude for second pulse has to be zero.

In Fig. 6.1, full HHG spectra is plotted for parameter corresponding to optimization of desired harmonic (51^{st}) using genetic algorithm (GA) by mixing two color lasers ($\omega, 3\omega$). The spectra in the left part of the Fig. 6.1, is calculated for the parameter obtained by optimization for beyond DA and right part of the figure, for the parameter obtained by optimization in within DA regime, whereas middle part is for unoptimized parameter. In all these three cases above part of the plot is calculated in within DA regime and below part is calculated beyond DA regime from the optimized parameter. The amplitudes of the lasers are used as optimization parameters. It has been shown that with two color laser optimization, harmonics intensities are enhanced by order of magnitude. The experiments usually have achieved better optimization than that of theoretical investigations. It can be seen that better optimization is achieved in the case of BDA regime. Hence the experimental results can be better explained in BDA regime.

In Fig. 6.2 (left), we have plotted the HHG spectra with the parameter obtained for 52^{nd} harmonic optimization. In middle part of Fig. 6.2, we have plotted the HHG spectra with the parameter obtained for 51^{st} harmonic optimization. and in the right part HHG spectra is for without optimization. And it can be observed

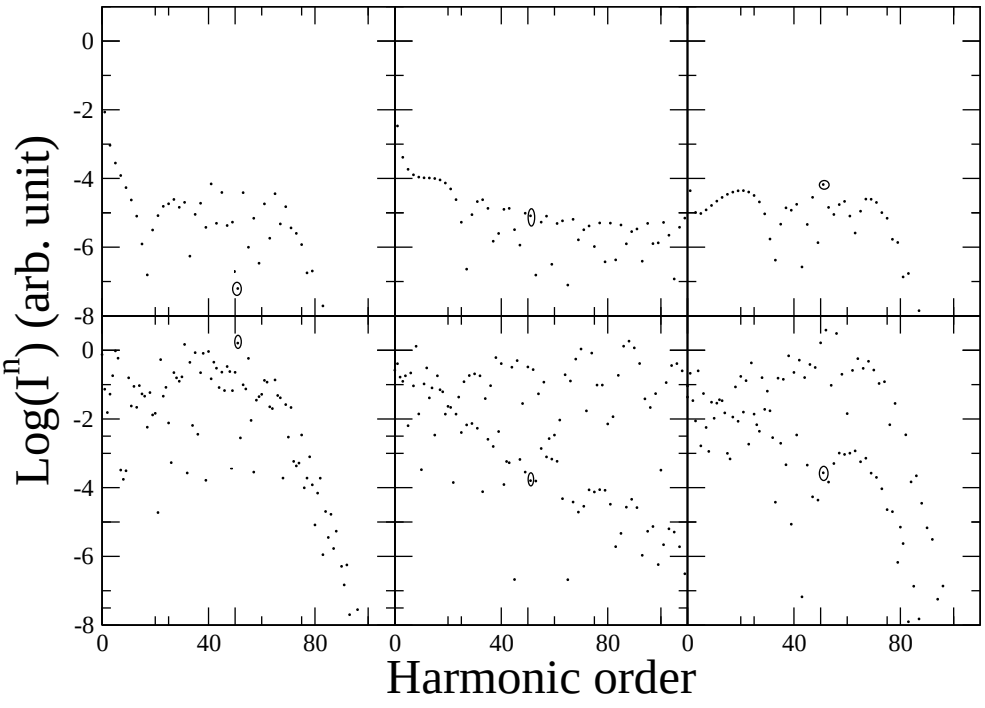

Figure 6.1: HHG spectra in the case of beyond dipole approximation (left) , no optimization (middle) and within dipole approximation (right) using two color laser $(\omega, 3\omega)$ with amplitudes optimized for 51^{st} harmonic within dipole approximation (above) and beyond dipole approximation (below).

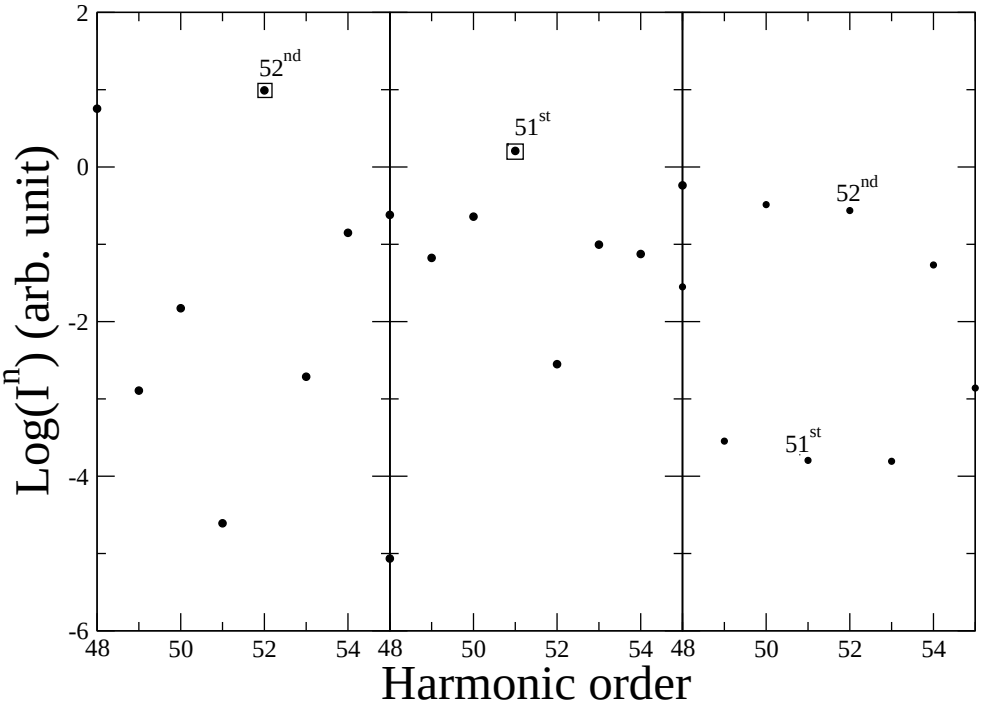

Figure 6.2: HHG spectra in the case of beyond dipole approximation with amplitudes optimized, for 52^{nd} harmonic (left), for 51^{st} harmonic (middle) and no optimization (right). Optimized harmonics are encircled.

that when odd order harmonic (51^{st}) are optimized the intensity difference between even and odd order harmonic is limited to the order of 3.5 only but when even order (52^{nd}) harmonic is optimized, the the intensity difference between even and odd order harmonic is found to be upto the order of 6. So from this study it can be inferred that if one needs even order harmonics ore intense than the odd order harmonics then he should optimize even order harmonics in beyond DA regime.

We would like to emphasize here that in each and every case better optimization is achieved in BDA regime with respect to DA regime. The better optimization in the case of BDA can be understood as follows: Rather than optimizing the laser parameter, lets write wave function at $t = 0$ as,

$$\psi = \sum c_i \phi_i$$

And optimize c_i which gives best desired harmonics. Then one can calculate the required laser parameters for which the desired wave function can be achieved, a much harder problem to solve. It is clear that as the number of term in the sum increases, the better optimization will be achieved. In the case of DA as shown by entropy plot only two non zero terms contribute. On top of that in case of BDA non dipole mechanism contribute to high harmonic generation optimization. So it is clear that BDA produces better optimization.

So it easily can be inferred that beyond DA plays a key role in optimization too along with giving rise to even order harmonics. It is found that increment in the intensity of the optimized harmonic is upto 10 times in the case of DA, and upto 458 times in the case of beyond DA so We can say that beyond dipole approximation plays an important role in optimization of selected harmonic. The optimization done beyond dipole approximation provides better explanation of the experimental results.

6.4 Summary

In summary, we have shown that although GA optimizes the intensity of a desired harmonic in any case of DA or beyond DA but the beyond dipole interaction term plays an important role in optimization process and it can enhance the intensity of selected harmonic quite efficiently by many times. And the difference between the intensity of even order and odd order harmonic is raise upto the order of 6 in the case of optimization of even order harmonics in beyond DA. We have presented the results of 51^{th} and 52^{nd} harmonic only but it is checked for many other harmonics too. This difference in intensity between even order and odd order harmonics is limited upto the order of 3.5 only in the case of optimization of odd order harmonics.

Bibliography

[1] H. Niikura, F. Lgar, R. Hasbani1, A. D. Bandrauk, M. Y. Ivanov1, D. M. Villeneuve1, and P. B. Corkum1 *Nature (London)*, vol. 417, p. 917, 2002.

[2] Y. Mairesse, A. de Bohan, L. J. Frasinski, H. Merdji, L. C. Dinua, P. Monchicourt, P. Breger, M. Kovacev, R. Taeb, B. C. H. G. Muller, P. Agostini, and P. Salires *Science*, vol. 302, p. 1540, 2003.

[3] T. U. A. Baltuka1, M. Uiberacker, M. Hentschel, E. Goulielmakis, C. Gohle, R. Holzwarth, V. S. Yakovlev1, A. Scrinzi1, T. W. Hnsch, and F. Krausz1 *Nature (London)*, vol. 421, p. 611, 2003.

[4] A. B. H. Yedder, C. L. Bris, O. Atabek, S. Chelkowski, and A. D. Bandrauk *Phys. Rev. A*, vol. 69, p. 041802, 2004.

[5] R. A. Bartels, M. M. Murnane, H. C. Kapteyn, I. Christov, and H. Rabitz *Phys. Rev. A*, vol. 70, p. 043404, 2004.

[6] P. Villoresi, S. Bonora, M. Pascolini, L. Poletto, G. Tondello, C. Vozzi, M. Nisoli, G. Sansone, S. Stagira, and S. D. Silvestri *Optics Letters*, vol. 29, p. 207, 2004.

[7] J. Xiao, Z. Sun, X. Zhang, Y. Wang, W. Zhang, Z. Wang, R.Li, and Z. Xu *J. Opt. Soc. Am. B*, vol. 23, p. 771, 2006.

[8] X. Chu and S.-I. Chu *Phys. Rev. A*, vol. 64, p. 021403, 2001.

[9] D. Yoshitomi, J. Nees, N. Miyamoto, T. Sekikawa, and T. K. G. M. S. Watanbe *Applied Physics B: Lasers and Optics*, vol. 78, p. 275, 2004.

[10] R. Bartels, S. Backus, E. Zeek, L. Misoguti, G. Vdovin, I. P. Christov, M. M. Murnane, and H. C. Kapteyn1 *Nature (London)*, vol. 406, p. 164, 2000.

[11] O. Boyko, C. Valentin, B. Mercier, C. Coquelet, V. Pascal, E. Papalazarou, G. Rey, and P. Balcou1 *Phys. Rev. A*, vol. 76, p. 063811, 2007.

[12] Y. Peng and H. Zeng *Phys. Rev. A*, vol. 78, p. 033821, 2008.

[13] A. D. Bandrauk and H. Z. Lu *Phys. Rev. A*, vol. 73, p. 013412, 2006.

[14] M. Klaiber, K. Z. Hatsagortsyan, and C. H. Keitel *Phys. Rev. A*, vol. 71, p. 033408, 2005.

[15] A. D. Bandrauk, O. F. Kalman, and T. T. N. Dang *J.Chem.Phys.*, vol. 84, p. 12, 1986.

[16] M. Forre, S. Selsto, J. P. Hansen, T. K. Kjeldsen, and L. B. Madsen *Phys. Rev. A*, vol. 76, p. 033415, 2007.

[17] M. W. Walser, C. H. Keitel, A. Scrinzi, and T. Brabec *Phys. Rev. Lett.*, vol. 85, p. 5082, 2000.

[18] A. Staudt and C. H. Keitel *J. Phys. B: At. Mol. Opt. Phys.*, vol. 36, p. 203, 2003.

[19] P. B. Corkum *Phys. Rev. Lett.*, vol. 71, p. 1994, 1993.

[20] M. Forre, J. P. Hansen, L. Kocbach, S. Selsto, and L. B. Madsen *Phys. Rev. Lett.*, vol. 97, p. 043601, 2006.

[21] L. B. Madsen and D. Dimitrovski *Phys. Rev. A*, vol. 78, p. 23403, 2008.

[22] M. Forre, S. Selsto, J. P. Hansen, and L. B. Madsen *Phys. Rev. Lett.*, vol. 95, p. 043601, 2005.

[23] N. J. Kylstra, R. A. Worthington, A. Patel, P. L. Knigh, J. R. V. de Aldana, and L. Roso *Phys. Rev. Lett.*, vol. 85, p. 1835, 2000.

[24] R. E. Wagner, Q. Su, and R. Grobe *Phys. Rev. Lett.*, vol. 84, p. 3282, 2000.

[25] S. X. Hu and C. H. Keitel *Phys. Rev. Lett.*, vol. 83, p. 4709, 1999.

[26] R. Taeb, V. Vniard, and A. Maquet *Phys. Rev. Lett.*, vol. 81, p. 2882, 1998.

[27] S. Patchkovskii, Z. Zhao, T. Brabec, and D. M. Villeneuve1 *Phys. Rev. Lett.*, vol. 97, p. 123003, 2006.

[28] S. Kazamias, D. Douillet, F. Weihe, C. Valentin, A. Rousse, S. Sebban, G. Grillon, F. Auge, D. Hulin, and P. Balcou *Phys. Rev. Lett.*, vol. 90, p. 193901, 2003.

[29] G. Tempea and T. Brabec *Appl. Phys. B*, vol. 70, p. 197, 2000.

Chapter 7

Conclusions

First we have shown that the beyond dipole interaction can fundamentally change the HHG spectra even if electron is confined into a space of $8\mathring{A}$ only during the interaction. The even order harmonics are found to be more intense even if only two monomer units of ethylene are included in model system. With increase in laser intensity the DA become more worse and near the cutoff even harmonics are many order high intense than the odd order harmonics. We conclude that dipole approximation is not valid while solving the time-dependent Schrodinger equation governing the behaviour for model polyacetylene system.

Next We have shown that the study of entropy during HHG provides interesting insight about molecular population dynamics. As it is shown that both HHG and entropy spectra changes fundamentally in the case of beyond DA. When all type of the harmonics (even as well as odd) is generated even if electron is confined into a space of $8\mathring{A}$ only during the interaction. We observe the significant increase in entropy in the case of beyond DA regime. These observation strongly support the non validity of DA during the process. So we conclude that dipole approximation is not valid while solving the time-dependent Schrodinger equation governing the behaviour

for model polyacetylene system.

Then we have shown that in the case of within dipole approximation regime and for linearly polarized laser light, due to dynamical symmetry, x polarized even order harmonics and y polarized odd order harmonics are produced. But in the case of beyond dipole approximation all the harmonics are emitted. When we use circularly polarised laser light is used, in either the case of DA or BDA, due to dynamical symmetry only allowed $5n \pm 1$ harmonics are produced.

And also we have shown that although GA optimizes the intensity of a desired harmonic in any case of DA or beyond DA but the beyond dipole interaction term plays an important role in optimization process and it can enhance the intensity of selected harmonic quite efficiently by many times. And the difference between the the intensity of even order and odd order harmonic is raise upto the order of 6 in the case of optimization of even order harmonics in beyond DA. This difference in intensity between even order and odd order harmonics is limited upto the order of 3.5 only in the case of optimization of odd order harmonics.

Finally We conclude this thesis by saying that dipole interaction term plays an vital role in both the process of HHG and the optimization as well. So dipole interaction term can not be ignored during solving TDSE for HHG.

7.1 Acknowledgement

This work has been supported by the ministry of Department of Sciences and Technology (DST), India. Its our pleasure to thanks to Prof. M. K. Mishra (I. I. T. Bombay, India) and Prof. Nimrod Moiseyev (Technion-Israel Institute of Technology, Haifa, Israel) for their valuable suggestion, and to the department of chemistry I. I. T. Guwahati for providing the fellowship.

PUBLICATIONS

1-Rajeev Mishra, Ashish K. Gupta, Even Order Harmonic Generation due to Beyond Dipole Approximation, (submitted)

2-Rajeev Mishra, Ashish K. Gupta, Study of Entropy during High harmonic generation, (under preparation)

3-Rajeev Mishra, Ashish K. Gupta, Dynamical Symmetry of Floquet State of CNT during HHG beyond dipole approximation, (under preparation)

4-Rajeev Mishra, Ashish K. Gupta, Optimization of HHG with adaptive control using an evolutionary search process, (under preparation)